AD-A106 517 NAVAL UNDERWATER SYSTEMS CENTER NEW LONDON CT NEW LO--ETC F/G 20/14
VLF/LF/MF WHISPERING GALLERY PROPAGATION STUDIES.(U)
SEP 81 P R BANNISTER
UNCLASSIFIED NUSC-TR-6503 NL

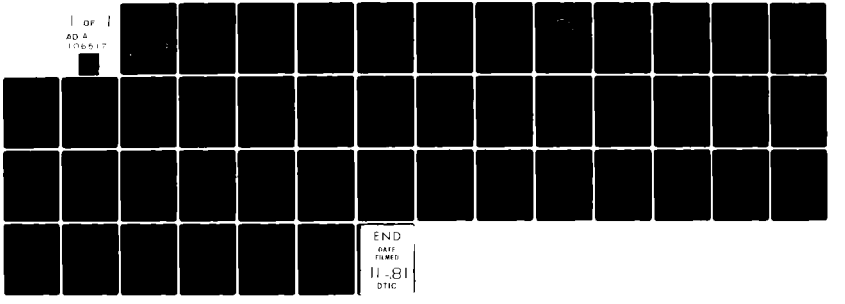

NUSC Technical Report 6503

9 September 1981

(15) LEVEL II

VLF/LF/MF Whispering Gallery Propagation Studies

Peter R. Bannister
Submarine Electromagnetic Systems Department

Naval Underwater Systems Center
Newport, Rhode Island / New London, Connecticut

Approved for public release; distribution unlimited.

Preface

This report was prepared under NUSC Project No. A59001, "Advanced Systems Concept" (U), Principal Investigator, Dr. D. A. Miller (Code 3491); Navy Program Element No. 11402 and Project No. X1083, Naval Electronics Systems Command, Communications Systems Project Office, Dr. D. C. Bailey (Code PME 110), Program Manager, Reconstitutable Communications, Dr. G. Brunhart (Code PME 110-11).

The Technical Reviewer for this report was Dr. D. A. Miller, Code 3491.

Reviewed and Approved: 9 September 1981

David F. Dence
Head, Submarine Electromagnetic Systems Department

The author of this report is located at the New London Laboratory, Naval Underwater Systems Center New London, Connecticut 06320.

REPORT DOCUMENTATION PAGE

READ INSTRUCTIONS BEFORE COMPLETING FORM

1. REPORT NUMBER	2. GOVT ACCESSION NO.	3. RECIPIENT'S CATALOG NUMBER
NUSC TR 6503		

4. TITLE (and Subtitle)

VLF/LF/MF WHISPERING GALLERY PROPAGATION STUDIES

5. TYPE OF REPORT & PERIOD COVERED

6. PERFORMING ORG. REPORT NUMBER

7. AUTHOR(s)

Peter R. Bannister

8. CONTRACT OR GRANT NUMBER(s)

9 Technical Reports

9. PERFORMING ORGANIZATION NAME AND ADDRESS

Naval Underwater Systems Center
New London Laboratory
New London, CT 06320

10. PROGRAM ELEMENT, PROJECT, TASK AREA & WORK UNIT NUMBERS

A59001

11. CONTROLLING OFFICE NAME AND ADDRESS

12. REPORT DATE

9 September 1981

13. NUMBER OF PAGES

38

14. MONITORING AGENCY NAME & ADDRESS (if different from Controlling Office)

15. SECURITY CLASS. (of this report)

UNCLASSIFIED

15a. DECLASSIFICATION / DOWNGRADING SCHEDULE

16. DISTRIBUTION STATEMENT (of this Report)

Approved for public release; distribution unlimited.

17. DISTRIBUTION STATEMENT (of the abstract entered in Block 20, if different from Report)

18. SUPPLEMENTARY NOTES

19. KEY WORDS (Continue on reverse side if necessary and identify by block number)

EM Propagation
Very Low Frequency (VLF)
Low Frequency (LF)
Medium Frequency (MF)
Whispering Gallery
Earth Ionosphere Waveguide

20. ABSTRACT (Continue on reverse side if necessary and identify by block number)

The propagation of very low frequency (VLF) and low frequency (LF) radio waves in the earth-ionosphere waveguide is affected profoundly by the earth's curvature. In particular, for frequencies greater than about 20 kHz, some modes are possible for which the energy is concentrated near the base of the ionosphere and the field strength near the ground is small. It is useful to think of such modes as being composed of waves repeatedly reflected at the inside surface of the ionosphere. Using analogy with sound waves, we

(over)

DD FORM 1 JAN 73 1473

403928

20. (Cont'd)

can call these modes whispering-gallery modes. Since they depend only very slightly on ground conductivity, these modes are also referred to as earth-detached modes.

The Navy currently is pursuing efforts leading to a feasibility demonstration of a balloon gateway communications system that would employ a balloon-to-balloon cross link based on the whispering-gallery propagation modes. This report discusses some recent whispering-gallery theoretical advances and simplifications.

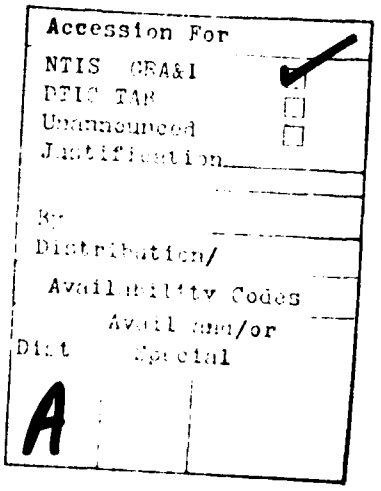

TABLE OF CONTENTS

LIST OF ILLUSTRATIONS

LIST OF ILLUSTRATIONS (Continued)

VLF/LF/MF WHISPERING-GALLERY PROPAGATION STUDIES

INTRODUCTION

Around the turn of the century, Lord Rayleigh[1-3] explained the efficient propagation of sound waves around the inside dome of St. Paul's Cathedral, in London, giving rise to a whispering-gallery effect. Between a speaker and a listener, both located close to the wall, an infinite family of sound ray paths exist, each having one or more reflections (almost at grazing incidence) off the surface of the dome. Since the travel time of the sound along each of these ray paths is similar, constructive interference and, hence, amplification takes place. In essence, an audible sound will travel around the inside of the dome with exceptionally low attenuation.

Analogs of the whispering gallery also occur within the earth, where the interface between two layers guides seismic rays in the same fashion as the dome guides acoustic rays.[4] Only the positions of the source and receiver differ from those in Lord Rayleigh's whispering gallery, both being located outside the layer interface at the earth's surface. The degree to which any particular interface acts as a whispering gallery depends on its ability to guide significant amounts of energy along its inner surface.

The propagation of very low frequency (VLF) and low frequency (LF) radio waves to considerable distances is conveniently treated by regarding the space between the earth and the ionosphere as a waveguide. Several authors have found that the least attenuated modes are affected profoundly by the earth's curvature. In particular, for frequencies greater than about 20 kHz, some modes are possible for which the energy is concentrated in a region near the base of the ionosphere and the field strength near the ground is small.[5-7] It is useful to think of such modes as being composed of waves repeatedly reflected at the inside spherical surface of the ionosphere, the rays being chords of this sphere (figure 1). Using analogy with sound waves, we can call these modes whispering-gallery modes. Since they depend only very slightly on ground conductivity, these modes are also referred to as earth-detached modes.

The Navy currently is pursuing efforts leading to a feasibility demonstration of a balloon gateway communications system that would employ a balloon-to-balloon cross link based on the whispering-gallery propagation modes.

The basic phenomenology of VLF and LF propagation is well known but the effects of high-altitude signal injection and reception are less well defined. In particular, the only experimental data available[8,9] are from a one-point two-frequency experiment which is insufficient for verification of the low frequency/medium frequency (LF/MF) whispering-gallery propagation mode. It is the purpose of this report to discuss some recent whispering-gallery theoretical advances and simplifications. Throughout this report, we will consider only propagation between vertical electric antennas over a sea water path.

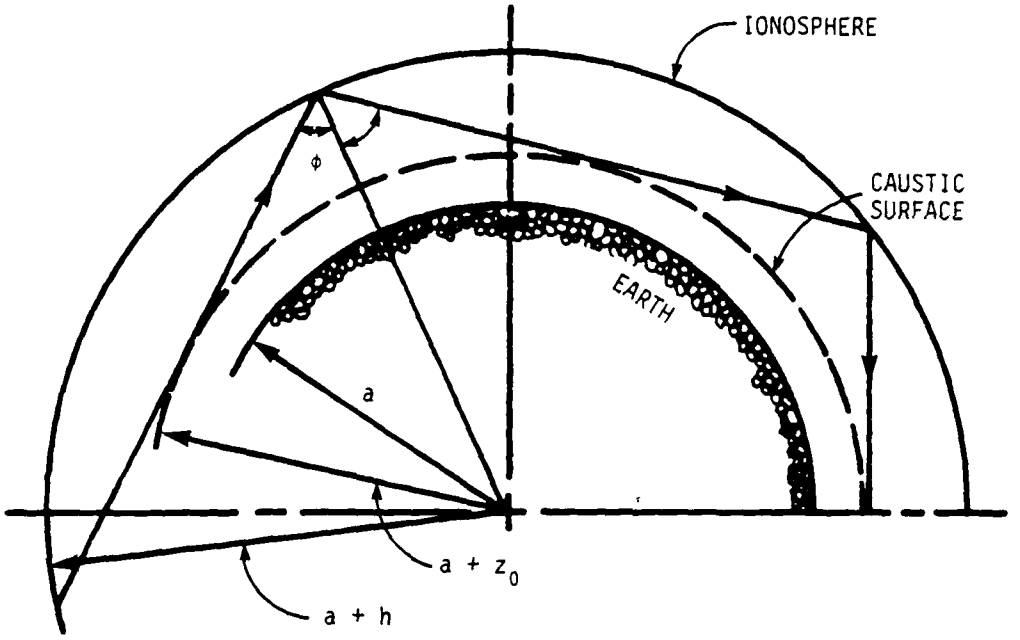

Figure 1. Whispering-Gallery Mode Description

PROPAGATION IN THE EARTH-IONOSPHERE WAVEGUIDE

The energy of propagating radio waves is confined principally to the shell between the earth and the ionosphere and this space is frequently denoted as the terrestrial waveguide. For long waves, the effective waveguide height, h, is comparable to a free-space wavelength, λ, and the characteristics of wave propagation are determined jointly by the properties of the two guide boundaries.

There are a number of propagating modes with distinct cutoff frequencies similar to those present in the microwave range. But, unlike the highly conducting guides of the microwave range, the upper boundary of the terrestrial waveguide is diffuse and a poor conductor; the finite conductivity of the earth's surface is also important. In the extremely low frequency (ELF) range, h is less than λ and only one waveguide mode propagates. For VLF, h exceeds λ and there are several propagating modes. In the LF range, the number of significant propagating modes may exceed 20.

Several field representations can be used to characterize the terrestrial propagation of radio waves. The fields in a uniform spherical shell between the earth and ionosphere can be expressed as a summation of spherical harmonics, which involves Legendre polynomials and spherical Bessel functions of integer order n. This series converges very slowly. The number of terms

required is of the order of 10 ka, where $k = 2\pi/\lambda$ and a is the earth's radius. Although this series is directly applicable in the ELF range, its exceedingly slow convergence may preclude its use at LF.

The Watson transformation changes the series of spherical harmonics into a residue or mode series, where the fields are expressed using Legendre functions and spherical Bessel functions of complex order ν. Each term of the mode series can be identified as an azimuthal wave propagating in the θ (= D/a) direction with a distinct phase velocity and attenuation rate.

Basically different is the geometric-optical series, where the individual terms are identified as a ground wave that propagates along the surface of the earth and sky waves that reach the receiver after a number of reflections from the ionosphere. This series provides results identical to those of the mode series for distances up to about 2 Mm.[10] The wave-hop propagation theory[11-15] extends the geometric-optical series to great distances (i.e., deep into the shadow region). The theory lends itself readily to physical interpretation, particularly in the propagation of LF pulses. Wave-hop techniques classically have been used in the LF band, principally for ground-to-ground transmissions. LF wave-hop calculations for elevated antennas[16] recently have been compared[17] successfully with mode-theory results.

The individual terms of the geometric-optical series corresponds to a sequence of waves that reach the receiver over different propagation paths. For pulse transmission, the individual delays of the received pulses correspond to the path lengths of the ground wave and the various sky waves. However, in the residue series, a number of modes have phase velocities (v) greater than the speed of light (c) and there is no one-to-one correspondence between the delay of the various pulses received and the phase velocities or the delay of the individual modes.

For the upper VLF and LF ranges (when the transmitter and receiver are located at or near the earth's surface), the lower order modes (where $v < c$) are excited very weakly. On the other hand, the higher order modes ($v > c$) are highly attenuated. Intermediate modes with $v \sim c$ dominate in the mode sum and the order of the dominant mode increases with increasing frequency.[18] Recent calculations[17] for 100 to 300 kHz daytime ground-to-ground propagation have shown relatively little modal structure, indicating that only a few modes are required.

When the transmitter and receiver are elevated to considerable heights (30 to 50 km), the height gain factors (HGF's) for the lower order modes ($v < c$) are substantial, even though the excitation factor is very weak. Thus, the modified HGF (i.e., the product of the excitation factor times the height gain of the transmitter times the height gain of the receiver) can be comparable to or greater than unity for these lower order least attenuated modes. However, for the upper LF frequencies, the daytime propagation mode structure is considerably more complicated for the elevated transmitter and receiver cases than it is for ground-to-ground propagation.[17] On the basis of mode theory, this would be anticipated since whispering-gallery type modes would become more influential with terminal elevation. On the basis of wave-hop theory, the added structure would be anticipated since more multipath possibilities exist when the terminals are elevated. For ground-to-ground transmission,

only one path applies to a single ionospheric reflection. However, when the terminals are elevated, there exist four paths, or hops, linking transmitter and receiver which correspond to a single ionospheric bounce.[1]

GENERAL THEORY

The phase integral form of the modal equation can be expressed as[7,19,20]

$$R_i \exp\left[-i2k\int_{z_0}^{h}\left(C_n^2 + 2z/a\right)^{1/2}dz + i\pi/2\right] = \exp(-i2n\pi) \ , \qquad (1)$$

where

R_i is the Fresnel reflection coefficient for vertically polarized waves incident on the ionospheric boundary at an angle of incidence ϕ (see figure 1,

$k = 2\pi/\lambda$,

$C_n = \cos\phi$,

a = earth's radius, and

$z_0 = -aC_n^2/2$.

The solution of equation (1) for the case where the earth and ionosphere are perfect reflectors is[7]

$$C_n^2 = \left[\frac{3\pi(n - 1/4)}{ka}\right]^{2/3} - \frac{2h}{a} \ . \qquad (2)$$

The attenuation rate, α_n, and the phase velocity, v_n, of mode n are given by

$$\alpha_n = k\,\mathrm{Im}C_n^2/2 \qquad (3)$$

and

$$v_n/C - 1 = \mathrm{Re}C_n^2/2 \ . \qquad (4)$$

There is a simple ray interpretation[7] of the modal equation, as illustrated in figure 1. The integral with limits z_0 and h is equal to the (complex) electrical length of a "to-and-fro" path between the caustic surface at $a + z_0$ and the ionospheric reflecting boundary at a + h. The quantity $\pi/2$ can be interpreted as the phase advance imparted as the "ray" grazes the caustic surface.

When the caustic surface is sufficiently elevated above the earth's surface, we would have a pure whispering-gallery mode of the type considered by Lord Rayleigh many years ago. Figure 2 is a plot of the height, z_0, versus frequency for the first five modes (for the case where the earth and ionosphere are perfect reflectors). The assumed ionospheric reflection height is 60 km. For the first order mode, z_0 is approximately equal to 10, 25, and 40 km at 25, 50, and 100 kHz, respectively.

We also notice from this figure that for frequencies of less than approximately 50 kHz there is, at most, one mode of the pure whispering-gallery type (for h = 60 km). However, as the frequency is increased there are more and more whispering-gallery modes. For example, at 100 kHz, three modes are present. Moreover, for frequencies in the MHz range, there would be so many whispering-gallery modes that no single mode would predominate. It is, then, preferable to abandon the waveguide mode treatment and to use a ray-tracing method.

In the region between the earth's surface and the height z_0, the field is evanescent. Consequently, excitation of these modes by a ground-based transmitter is very weak. This fact is borne out by the behavior of the first order mode excitation factor at the higher VLF frequencies and ionospheric reflection heights, where the phase velocity is less than the speed of light and the excitation factor decreases exponentially; that is,

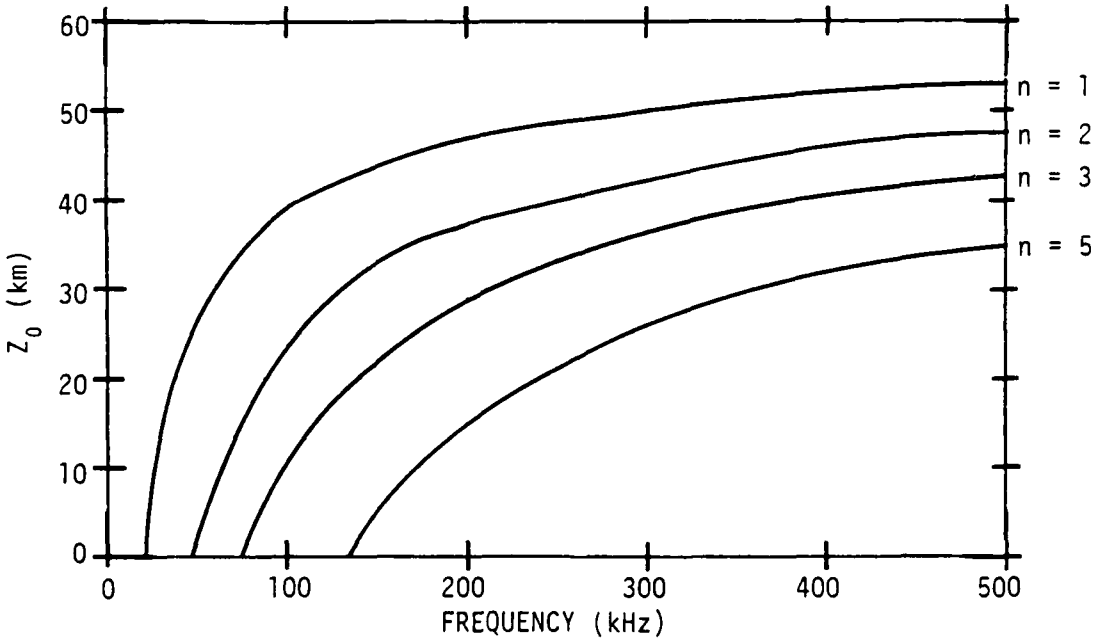

Figure 2. z_0 Versus Frequency for h = 60 km

$$A_n \sim \frac{y_0}{2t_n^{1/2}(y_0 - t_n)^{1/2}} \exp\left(-\frac{4}{3} t_n^{3/2}\right) , \tag{5}$$

where

$$t_n = (ka/2)^{2/3}(-C_n^2)$$

and

$$y_0 = (ka/2)^{2/3}(2h/a) .$$

The first order mode excitation factor[21] is plotted versus frequency in figure 3 for the case where the earth and ionosphere are perfect reflectors. For example, at a frequency of 30 kHz and an ionospheric reflection height of 80 km, the first order mode excitation factor is approximately -24 dB, while for h = 90 km, $A_1 \sim$ -36 dB.

On the other hand, while the excitation factor decreases exponentially, the HGF's for the transmitter, $G_n(z)$, and receiver, $G_n(\hat{z})$, increase exponentially; that is,

$$G_n(z) \sim \sqrt{\pi}\, t_n^{1/4} A_i(t_n - z) \exp\left(+\frac{2}{3} t_n^{3/2}\right) \tag{6}$$

and

$$G_n(\hat{z}) \sim \sqrt{\pi}\, t_n^{1/4} A_i(t_n - \hat{z}) \exp\left(+\frac{2}{3} t_n^{3/2}\right) , \tag{7}$$

where

$z = (ka/2)^{2/3}(2h_T/a)$,

$\hat{z} = (ka/2)^{2/3}(2h_R/a)$,

h_T is the transmitting antenna height,

h_R is the receiving antenna height, and

$A_i(t_n - z)$ is an Airy function, as defined by Miller[22] or Abramowitz and Stegun.[23]

For real arguments, this function peaks (= 0.535) at -1, oscillates for large negative arguments, and becomes exponentially small for large positive arguments.

$G_n(z)$ is plotted in figure 4 for the case where f = 100 kHz, h = 70 km, and the ionospheric conductivity is 10^{-6} S/m.[18] For this particular situation, the attenuation rates for the first five modes are all equal to about 3 dB/Mm, while the excitation factors are substantially different; that is, $A_1 \sim 4.3 \times 10^{-8}$, $A_2 \sim 7.4 \times 10^{-5}$, $A_3 \sim 1.1 \times 10^{-2}$, and $A_5 \sim 1.6$. The peaks

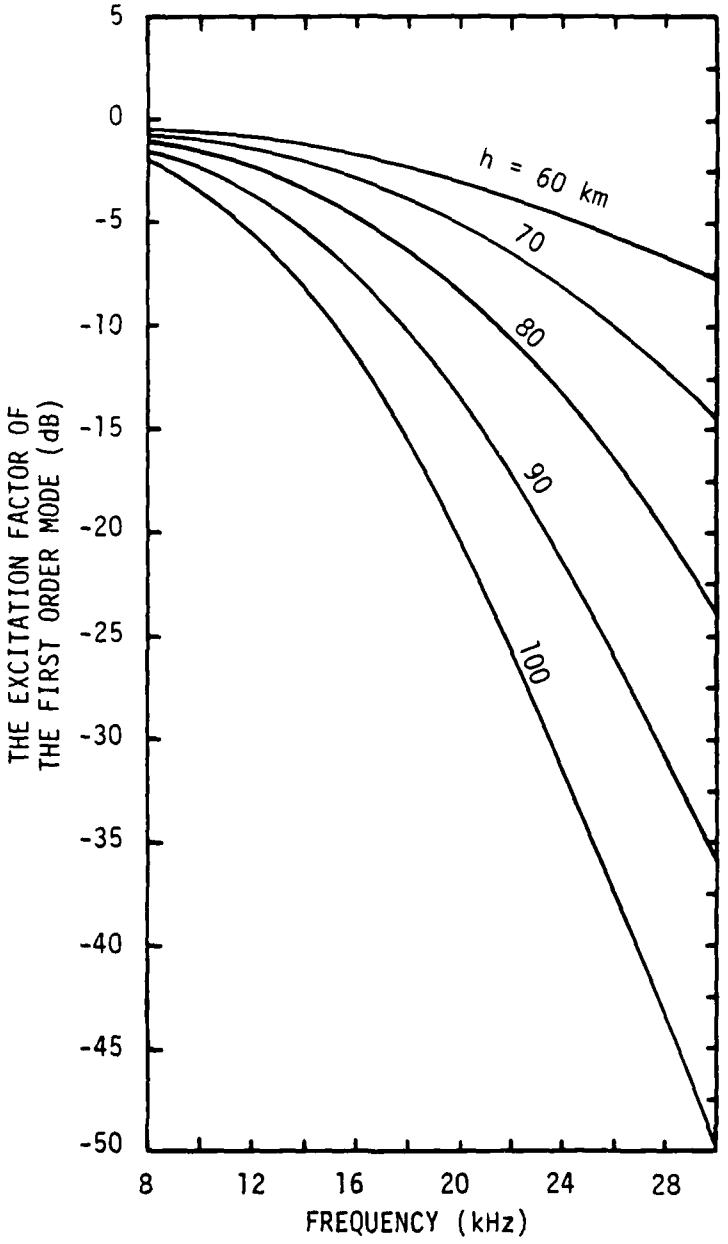

Figure 3. VLF First Order Mode Excitation Factor Versus Frequency for the Case Where Both the Earth and Ionosphere Are Perfect Reflectors

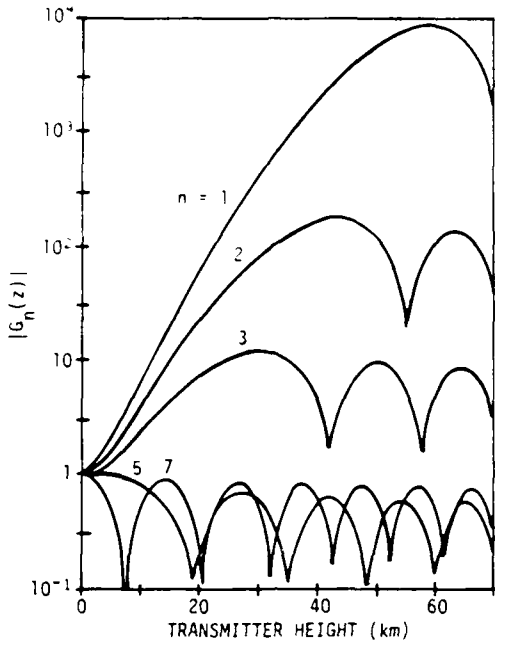

Figure 4. Typical HGF's of LF Waveguide Modes
(f = 100 kHz, h = 70 km, $\sigma_i = 10^{-6}$ S/m)

and valleys of the individual mode curves correspond to the maxima and minima of the Airy function $A_i(t_n - z)$. From this figure, we see that the height gains for the lower order modes can be substantial.

The modified HGF (i.e., the product of the excitation factor times the height gain of the transmitter times the height gain of the receiver) can be expressed as

$$HGF = \Lambda_n G_n(z) G_n(\hat{z}) \sim \frac{\pi y_0}{2(y_0 - t_n)^{1/2}} A_i(t_n - z) A_i(t_n - \hat{z}) \ . \qquad (8)$$

If both the transmitting and receiving antennas are sufficiently elevated, the modified HGF becomes comparable to or greater than unity. For example, referring to figure 4, we see that for $h_T = h_R = 40$ km, the height gain for the second order mode $G_2(z) = G_2(\hat{z}) \sim 150$. Since $\Lambda_2 \sim 7.4 \times 10^{-5}$, HGF ~ 1.7. Thus, while it is extremely difficult to excite these earth-detached modes from a ground-based transmitter, the advantages of exciting the least attenuated modes by elevated sources can be significant.

The vertical electric field strength produced by a vertical electric antenna located in the earth-ionosphere waveguide can be expressed as[18-21]

$$E_v \sim \frac{300}{h}\left[\frac{P_R\lambda}{a \sin D/a}\right]^{1/2} \sum_n \Lambda_n G_n(z) G_n(\hat{z}) \exp\left[-\frac{\alpha_n D}{10^6}\right] \text{ V/m} , \qquad (9)$$

where all lengths are in meters and the radiated power, P_R, is in kilowatts.

Once a particular ionospheric conductivity model is assumed, the individual parameters of equation (9) (excitation factor, height gain, phase velocity, and attenuation rate) can be calculated for each mode and summed. Unfortunately, in the LF range, the number of modes to be summed may exceed 20.

The Navy recently has funded the General Electric Company (GE) to establish an adequate computer model to facilitate high-altitude signal injection and reception analysis at frequencies from approximately 15 to 500 kHz through modifications of the existing Defense Nuclear Agency (DNA) sponsored weapons effects on D-region communications (WEDCOM) computer model.[24-30] WEDCOM has both LF ray theory and VLF waveguide computational codes that can be selected for utilization depending on the particular frequency to be analyzed. Detailed information on the WEDCOM models and the extensive modifications implemented to facilitate high-altitude injection and reception propagation computations can be obtained from the GE TEMPO personnel at Santa Barbara, CA. The main result of their analysis is that LF communications over sea water between high-altitude transmitters and receivers is feasible in both normal and nuclear-disturbed environments.

SIMPLIFIED APPROXIMATE THEORY

One drawback of computer simulations is that they often provide little physical insight into the various propagation parameters. However, by employing a combination of ray and mode theory, the following simplified whispering-gallery propagation equation can be obtained:

$$E_v \sim -12.2 + 10 \log P_R + G - 5 \log aw - 10 \log(a \sin D/a) - \alpha D + \text{HGF dBV/m} . \qquad (10)$$

This approximate expression for the vertical electric field produced by a vertical electric antenna (which is a slight variation of equation (26) of reference 27) provides some physical insight into the various propagation parameters.

The quantities that make up this expression are the radiated power P_R (in kW), antenna gain G, duct width w, spreading loss a sin D/a, dominant-mode attenuation rate α, and modified HGF. The spreading loss is easily determined and the maximum duct width is equal to the distance between the earth and ionosphere (approximately 60 to 90 km).

For P_R = 1 kW, G = 1.8 dB, w = h = 60 km, 5 log aw = -27.9 dB, and

$$E_v \sim -68.3 - 10 \log(a \sin D/a) - \alpha D + HGF \text{ dBV/m/kW} , \quad (11)$$

or

$$E_v \sim 51.7 - 10 \log(a \sin D/a) - \alpha D + HGF \text{ dB}\mu\text{V/m/kW} , \quad (12)$$

where a and D are both in Mm and α is in dB/Mm.

If w = h = 90 km, the constants in equations (11) and (12) become -69.2 and 50.8 dB, respectively. A few comparisons of equation (12) with mode-theory computer calculations are presented in the appendix.

The most important propagation parameter to be determined is the dominant-mode attenuation rate. Figure 5 is a plot of the 180 kHz measured field strength versus range.[31,32] From this figure, we see that there is a substantial difference between daytime and nighttime attenuation rates at the upper LF frequencies.

The propagation of VLF and LF radio waves to substantial distances is made possible by the high reflectivity of the lower ionosphere at oblique incidence. The latter is due to the relatively sharp gradient of the electron density in the D-region of the ionosphere. In fact, for many purposes, the assumption of an abrupt lower edge of the ionized region has permitted an analytical approach to the problem that has produced useful results. In the main, these are confirmed experimentally. However, a number of discrepancies have

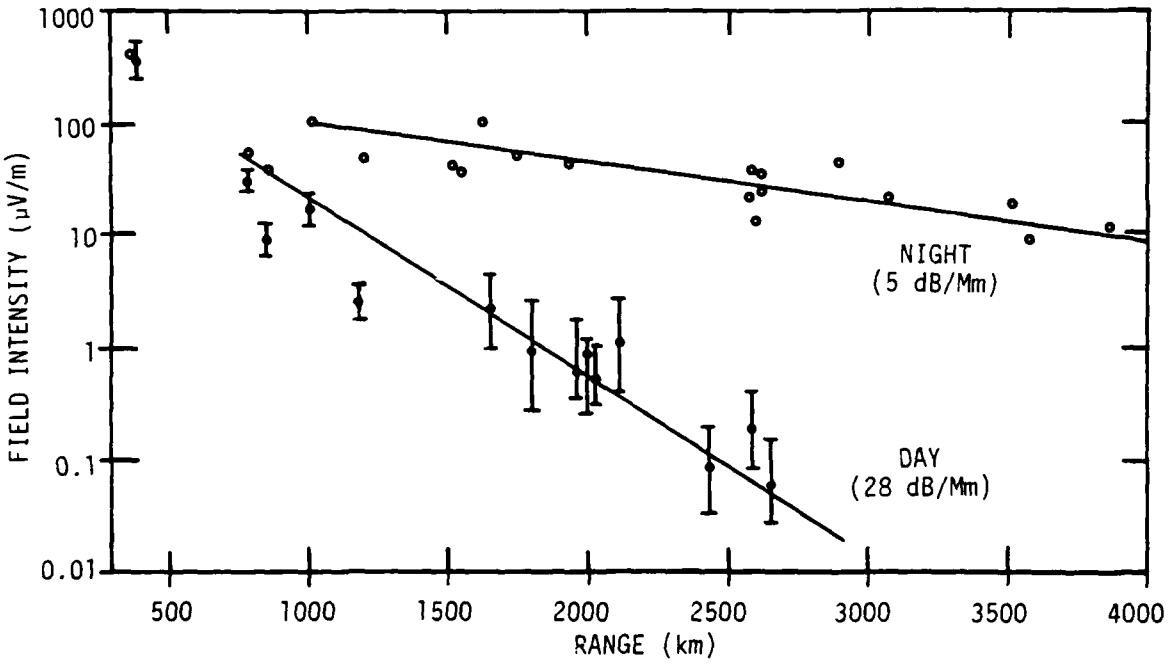

Figure 5. Measured Field Strength for 180 kHz Ground-to-Ground Transmission

been observed that suggest that the sharply bounded model is not entirely adequate.

During the past 20 years, evidence from a number of independent experimental approaches has indicated that the profile of the electron density (and ionospheric conductivity) in the lower ionosphere can be described approximately by an exponential function of height.

For horizontal polarization, the reflection loss for an exponentially varying ionospheric conductivity profile is a function of frequency, angle of incidence, and ionospheric conductivity gradient β.[21] For vertical polarization, the relationship is more complex. β is the length over which the conductivity changes by a ratio of 2.71; it is that reciprocal of Wait's β factor.[21] (That is, the commonly employed daytime β value of 0.3 km^{-1} corresponds to an β of 3.33 km.) The magnitude of the reflection loss for vertical polarization is presented in figure 6 as a function of frequency;[33] $\cos \phi$ = 0.16, which is the case for grazing incidence at the earth's surface. The straight-line portions of the theoretical curves are also valid for horizontal polarization. Typical values of β in the VLF/LF range are 0.5 to 2 km at night and 2 to 3.33 km during the day.

It should be noted that the ionospheric conductivity gradient of importance is the value of β at the ionospheric reflection height H_R. Typical values of H_R in the VLF/LF range are 55 to 70 km during normal daytime propagation conditions and 75 to 90 km during normal nighttime propagation conditions. The major reflection height usually can be determined by examining the detailed vertical field structure[25,34-40] (i.e., H_R equals the height where the downcoming horizontal magnetic field strength component is reduced by a factor of 2). A simpler method,[41] which is actually quite accurate for many cases, is that the reflection height is located at the height where the ratio of the ionospheric conductivity parameter[21] ω_r to ω is equal to $\sqrt{2} \cos^2 \phi$; that is,

$$H_R \sim H - \beta \ln\left(\frac{2.5 \times 10^5}{\sqrt{2}\ \omega \cos^2 \phi}\right), \tag{13}$$

where H is the exponential ionospheric conductivity profile reference height.

The formula for the ionospheric reflection loss for horizontal polarization is[21]

$$|R| \sim \exp[-(2\pi^2 \beta/\lambda) \cos \phi] . \tag{14}$$

As we previously mentioned, the reflection loss is a function of frequency, angle of incidence, and ionospheric conductivity gradient. Since the whispering-gallery mode attenuation rate is equal to the reflection loss (which varies as $\cos \phi$) divided by the distance between reflections, d_1 (which also varies as $\cos \phi$), the attenuation rate is independent of the angle of incidence and is just a function of frequency, ionospheric conductivity gradient, and radius of the earth. That is,

$$\alpha = \frac{|R|}{2d_1} = \frac{|R|}{2a \cos \phi} \tag{15}$$

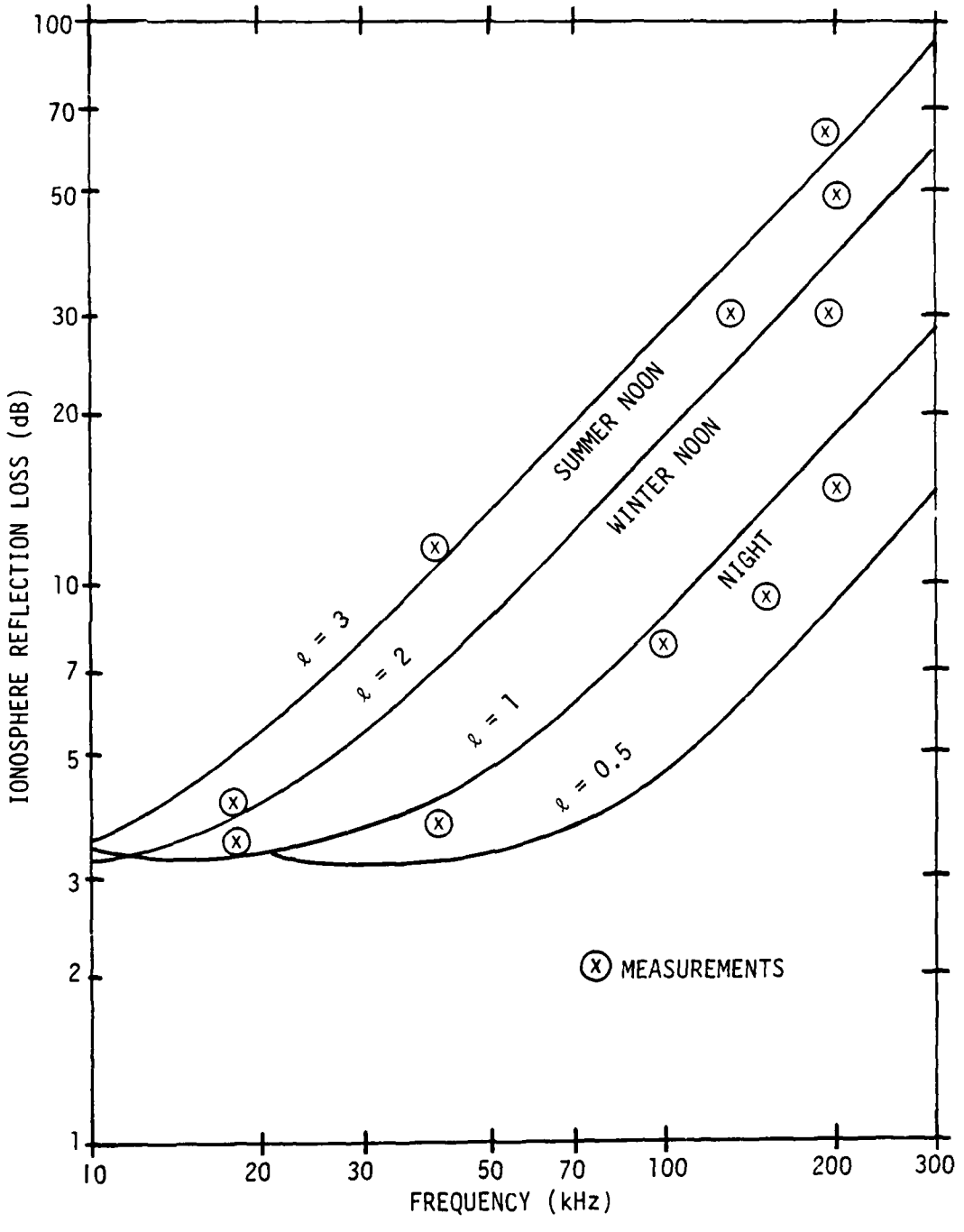

Figure 6. Ionospheric Reflection Loss Versus Frequency (cos ϕ = 0.16)

or, in dB/Mm,

$$\alpha \sim \frac{-8.686 \times 10^6}{2a}\left(\frac{2\pi^2 \ell}{\lambda}\right) \sim 13.4(\ell/\lambda) \ . \tag{16}$$

Based on an analysis of about 30 years of 10 to 100 kHz propagation data, Pierce[42] devised the following empirical formula for the attenuation rate α that had α varying as the frequency to some power u:

$$\alpha \sim \frac{8.686 \times 10^6}{a}(0.1\ f_{kHz})^u \ \text{dB/Mm} \ , \tag{17}$$

where, for propagation over a sea water path, u ~ 0.5 to 0.6 at night and 0.9 to 1.0 during the day.

We will now take the attenuation-rate formula that was obtained from the reflection loss (equation (16)) and modify it so that both the frequency and gradient vary as some power u; that is, let

$$\alpha \sim 13.4(\ell/\lambda)^u = 13.4\left(\frac{\ell f_{kHz}}{300}\right)^u \ \text{dB/Mm} \ . \tag{18}$$

If we take typical daytime values of ℓ = 2.5 km and u = 0.9, the resulting daytime attenuation-rate formula

$$\alpha_D \sim 0.18 f_{kHz}^{0.9} \ \text{dB/Mm} \tag{19}$$

is almost identical to Pierce's empirical result[42] of

$$\alpha_D \sim 0.17 f_{kHz}^{0.9} \ \text{dB/Mm} \ . \tag{20}$$

If we take a typical nighttime value of ℓ = 1 km, the resulting nighttime attenuation-rate formula is also very close to Pierce's empirical result.[42]

We will now compare our attenuation-rate formula (equation (18)) with the results obtained from some GE computer simulations.[24,27,28] For the comparison presented in figure 7, the slope of the daytime ionospheric conductivity profile was 2.5 km while the nighttime gradient was 0.5 km. The circles are the computer simulation results while the curves are the attenuation rates determined from equation (18). Following Pierce,[42] u was assumed to be 0.9 during the day and 0.6 at night. Note that there is excellent agreement between the approximate dominant-mode attenuation-rate formula and the computer simulation results.

Figure 8 is a similar comparison for the case where the daytime gradient employed was 3.33 km while the nighttime gradient was 1 km. Again, the agreement is excellent. Note that, as the frequency is increased, there is a substantial difference between daytime and nighttime attenuation rates. For example, at 400 kHz the daytime attenuation rate is approximately 50 dB/Mm while the nighttime attenuation rate is only 15 dB/Mm.

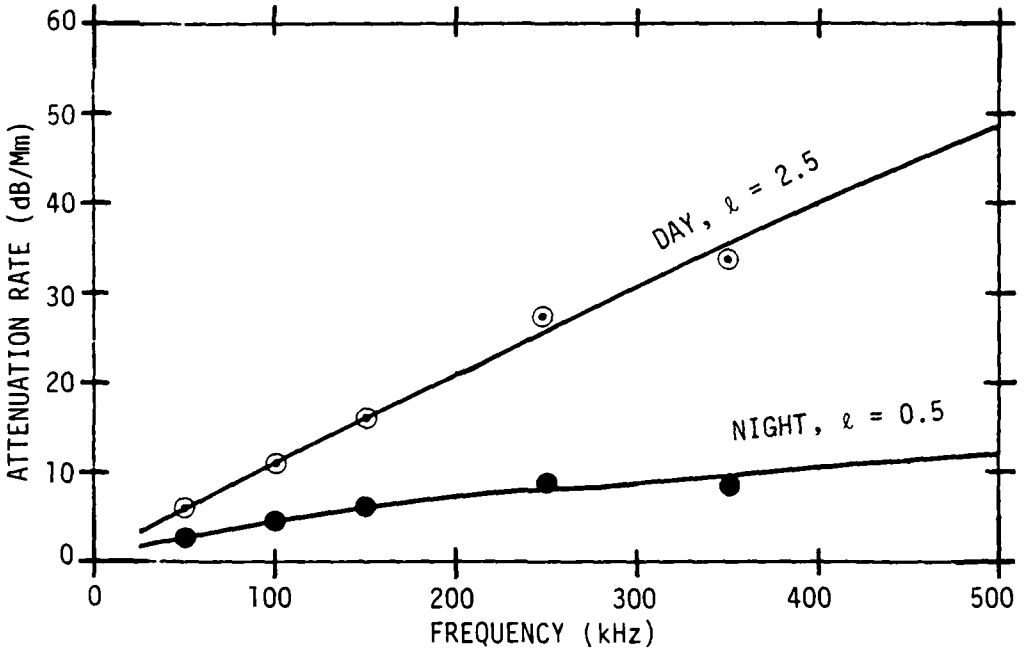

Figure 7. Comparison of Attenuation Rate Versus Frequency (Daytime ℓ = 2.5 km and Nighttime ℓ = 0.5 km)

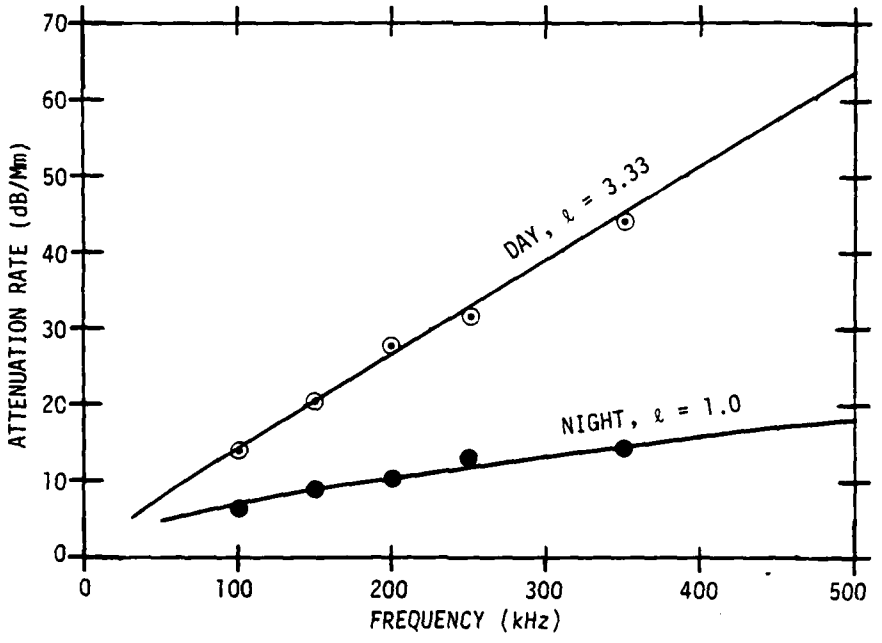

Figure 8. Comparison of Attenuation Rate Versus Frequency (Daytime ℓ = 3.33 km and Nighttime ℓ = 1.0 km)

A comparison of the modified HGF versus frequency is presented in figure 9. (The transmitting and receiving antennas are assumed to be located at heights around 30 to 40 km.) These approximate values were determined with the help of the computer simulations. Here, again, we see substantial differences between daytime and nighttime propagation at the higher frequencies. For example, at 400 kHz, the HGF is only about 10 dB at night but is near 30 dB during the day. However, this daytime HGF is easily offset by the substantial daytime attenuation rate of 40 to 50 dB/Mm. Moreover, since many whispering-gallery propagation modes will be present at the higher LF and lower MF frequencies, the model interference pattern will be severe.

Since we have now determined the various inputs to the simplified whispering-gallery propagation equation, we will put it to a test. An experiment was conducted[8,9] in May 1972 that consisted of low power (approximately 50 W) transmissions on 219 and 438 kHz between balloons spaced 1.6 Mm apart hovering for over 30 hr at altitudes of 30 to 37 km. Ground-to-ground as well as balloon-to-balloon signals were simultaneously measured for comparison of path loss. The balloon-to-balloon measured field strengths were 40 to 60 dB higher than the ground-to-ground measured field strengths.

Figure 10 shows a comparison of the measured and predicted balloon-to-balloon field strengths. The spread in the predicted value is due solely to the variation in the ionospheric conductivity gradient assumed. The higher daytime predictions correspond to a gradient of 2 km while the lower predictions are for ℓ = 3.33 km. The higher nighttime field strength predictions are based on a gradient of 0.5 km while the lower predicted value assumes ℓ = 2.0 km. Since the measured and predicted intervals overlap, we see that the measured field strengths can be explained satisfactorily in terms of realistic

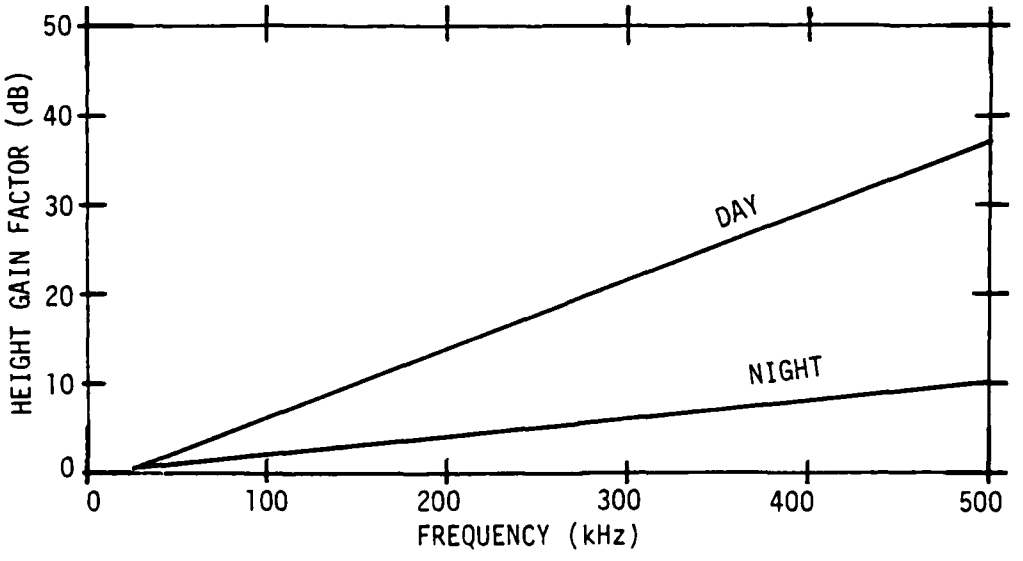

Figure 9. Approximate HGF Versus Frequency
($h_T = h_R$ = 30 to 40 km)

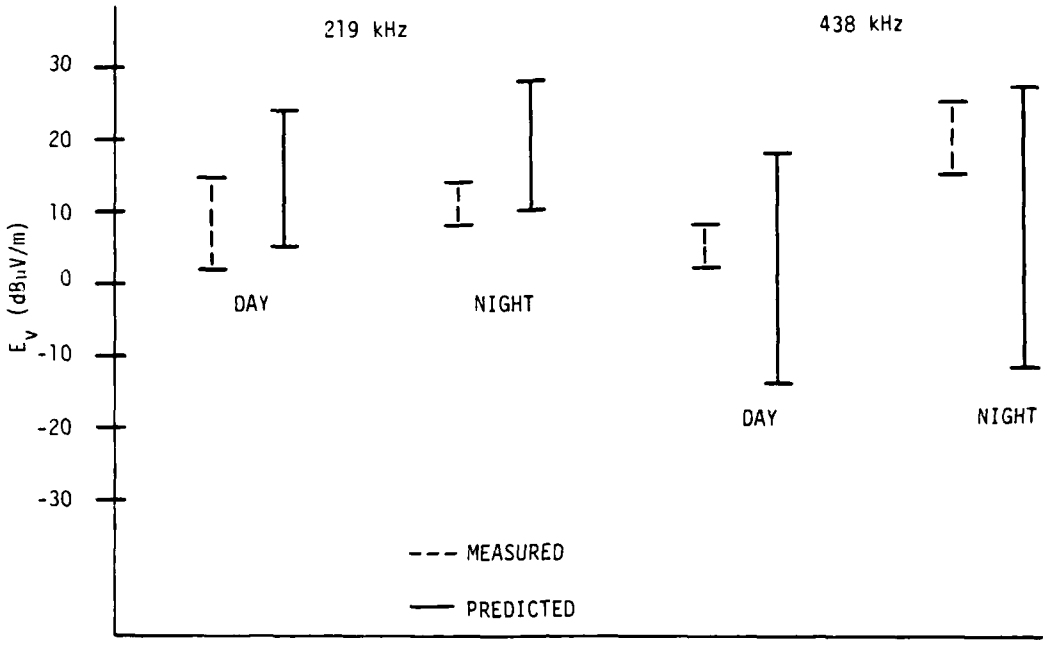

Figure 10. Comparison of Measured and Predicted Field Strengths for the Balloon-to-Balloon May 1972 Whispering-Gallery Propagation Experiment

ionospheric conductivity parameters. However, the large spread also points out the need to measure simultaneously the ionospheric conductivity profile during a whispering-gallery propagation experiment.

A plot of the predicted nighttime field strength versus range for the case where the gradient is 1 km is presented in figure 11. The attenuation rate varies from 3 dB/Mm at 25 kHz to 16 dB/Mm at 400 kHz. The radiated power is 1 kW and autumn nighttime noise conditions[43] are assumed. The circles represent the range where the signal-to-noise ratio (SNR) is 0 dB in a 1 Hz bandwidth. Note that this range varies from 10.5 Mm at 25 kHz to 5 Mm at 400 kHz.

Figure 12 is a plot of the predicted daytime field strength versus range for the case where the ionospheric conductivity gradient is 2.5 km. The attenuation rate varies from 3.5 dB/Mm at 25 kHz to 40 dB/Mm at 400 kHz. Again, the radiated power is 1 kW and autumn daytime noise conditions[43] are assumed. Note that the 0 dB SNR (in a 1 Hz bandwidth) range varies from 11 Mm at 25 kHz to only 3 Mm at 400 kHz. These last two figures clearly point out the advantages of employing frequencies of less than 100 kHz for long-distance whispering-gallery propagation.

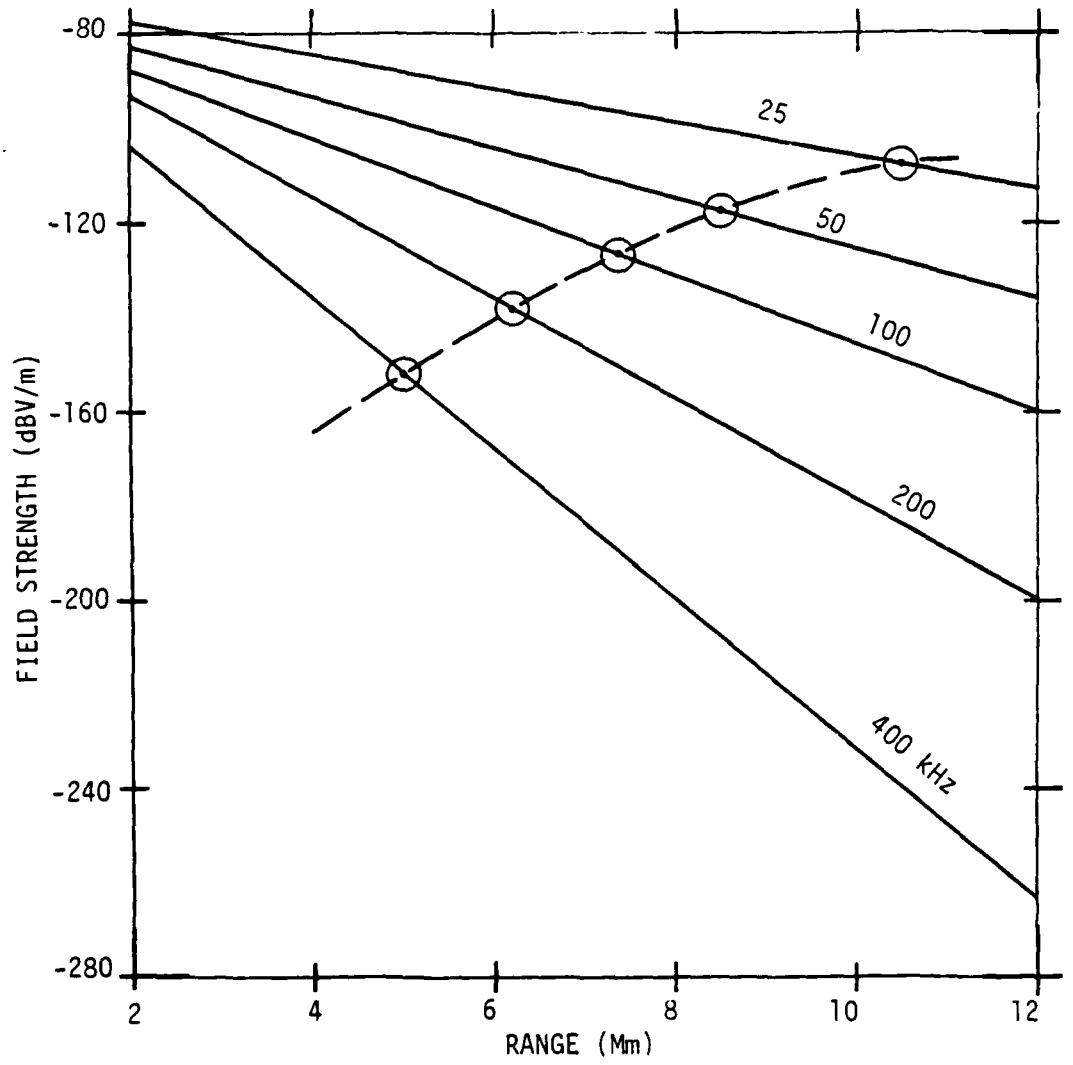

Figure 11. Predicted Nighttime Field Strength Versus Range for Various Frequencies (ℓ = 1 km)

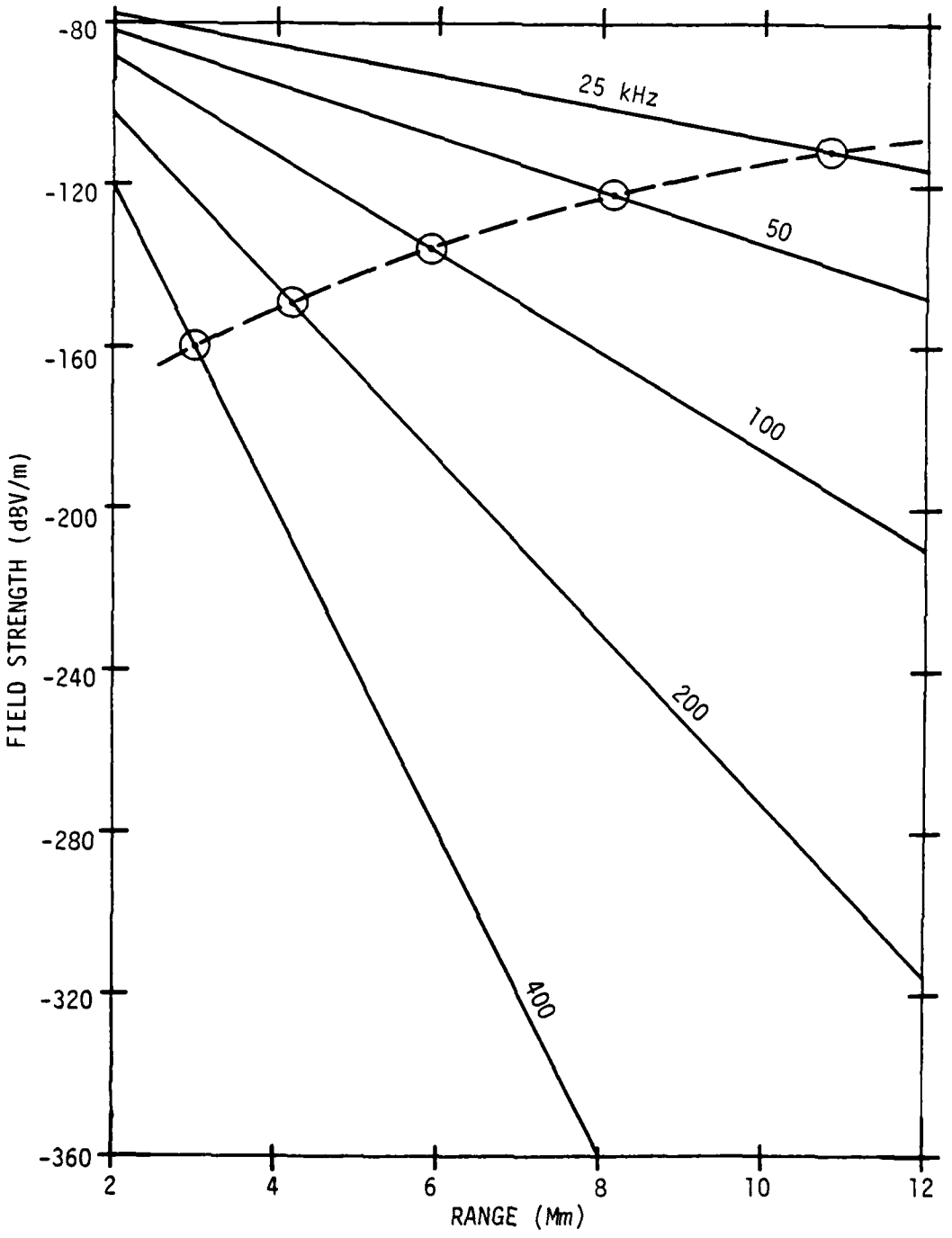

Figure 12. Predicted Daytime Field Strength Versus Range for Various Frequencies (ℓ = 2.5 km)

DISCUSSION

The upper VLF and lower LF frequencies (~ 25 to 50 kHz) not only have the advantage of lower attenuation rates but also the advantage of very few whispering-gallery modes, in some cases only one. Thus, the whispering-gallery propagation model interference pattern will be nowhere near as severe as it is at the higher LF and lower MF frequencies.

The principal unknown in the earth-ionosphere waveguide model is the ionospheric conductivity which is, in part, a function of the electron- and ion-density distribution with height. Fixed location sounding systems are somewhat inaccurate because the ionization densities are quite low in the region of importance to VLF and LF propagation.

Propagation studies using long path VLF/LF data provide an indirect but more useful description of the ionosphere for propagation prediction. Much success has been achieved with such studies by using an exponential electrons-only ionospheric profile specified by a gradient ℓ (= $1/\beta$) and a reference height H. On the basis of the analysis[44] of the latest experimental data, ℓ = 2.0 km and H = 70 km during summer daytime propagation conditions while ℓ = 3.33 km and H = 74 km for daytime propagation in the winter.

Figure 13 is a plot of the predicted 30 kHz ground-to-ground propagation field strength versus range for summer daytime propagation conditions (ℓ = 2.0 km, H = 70 km). The individual curves, labeled 1, 2, and 3, are the individual mode results while the curve labeled 1,2,3 is the resultant multiple-mode field

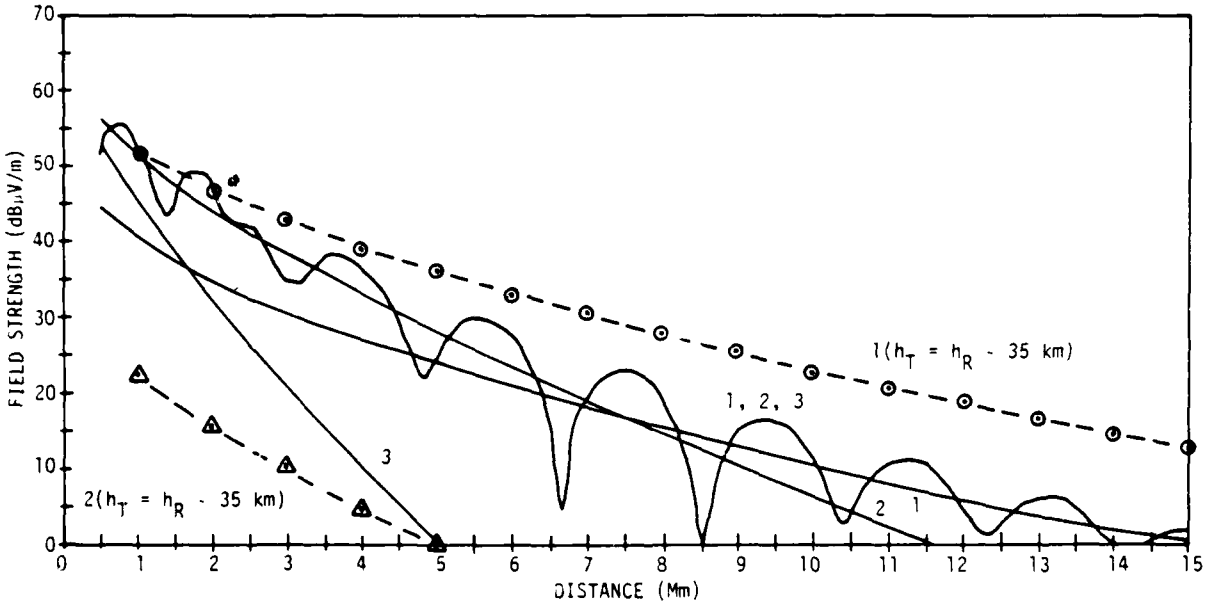

Figure 13. Predicted 30 kHz Ground-to-Ground and 35 km-to-35 km Field Strengths Versus Range for Typical Summer Daytime Propagation Conditions (ℓ = 2 km, H = 70 km, P_R = 1 kW)

strength. These curves were calculated[45] employing the following values for the various propagation parameters (as given by Wait and Spies[46]): α_1 = 2.34 dB/Mm; α_2 = 4.07 dB/Mm; α_3 = 9.53 dB/Mm; A_1 = -10.4 dB; A_2 = 2.6 dB; and A_3 = 1.8 dB.

Since the third order mode is highly attenuated, it is essentially negligible beyond about 3 Mm. However, the first and second order modes are comparable at all ranges, resulting in a substantial interference pattern, especially in the 5 to 10 Mm range.

Referring to Wait (pp. 379-389),[21] we see that for f = 30 kHz, h = 70 km, and h_T ~ 35 km, the HGF for the first order mode is $G_1(z) \sim 2.05$ (6.25 dB). On the other hand, the HGF for the second order mode, $G_2(z)$, is minimal at h_T ~ 35 km. If the ionosphere were a perfect reflector, $G_2(z)$ would be zero at h_T ~ 35 km. For ℓ = 2 km, $G_2(z) \simeq 0.2$ (-14.0 dB) at this height. Therefore, if both the transmitting and receiving antennas are located at a height of approximately 35 km, the modified HGF's are

$$(HGF)_1 = A_1 G_1(z) G_1(\hat{z}) \sim -10.4 + 6.25 + 6.25 = +2.1 \text{ dB} \qquad (21)$$

and

$$(HGF)_2 = A_2 G_2(z) G_2(\hat{z}) \sim +2.6 - 14.0 - 14.0 = -25.4 \text{ dB} . \qquad (22)$$

Also presented in figure 13 (the upper and lower curves) are the field strength versus distance plots for the first and second modes for the situation where both the transmitting and receiving antennas are located at a height of approximately 35 km. These plots were calculated using both the mode-theory and simplified approximate-theory equations (equations (9) and (12)). Both methods yielded nearly identical results (within 1 dB) at all ranges.

Since this first order pure whispering-gallery mode is clearly dominant, the model interference pattern will be negligible beyond approximately 2 Mm. The 35 km-to-35 km field strength is 3 to 30 dB greater than the ground-to-ground field strength (depending on range), with the average enhancement being approximately 12.5 dB for ranges greater than 9 Mm.

It should be noted that Bahar[47] has recently computed the VLF electromagnetic fields along the propagation path in an irregular spheroidal model of the earth-ionosphere waveguide using a full-wave approach. He has also pointed out the advantages of exciting the VLF earth-detached mode to minimize the effects of mode interference.

CONCLUSIONS

In this report we have discussed some recent theoretical advances and have developed a simplified approximate theory dealing with whispering-gallery (or earth-detached mode) propagation in the earth-ionosphere waveguide. We

have shown that the simplified approximate theory agrees remarkably well with mode-theory computer calculations.

We have also shown that the balloon-to-balloon measurement results obtained during the May 1972 whispering-gallery experiment can be explained in terms of realistic ionospheric conductivity profiles.

We have determined that substantial HGF's can be obtained at the higher LF and lower MF frequencies. However, they are offset by very high attenuation rates and severe modal interference patterns.

We have shown that the upper VLF and lower LF frequencies (approximately 25 to 50 kHz) are more favorable for whispering-gallery propagation. They not only have the advantage of lower attenuation rates but also the advantage of very few whispering-gallery modes, in some cases only one. Thus, the whispering-gallery modal interference pattern will be nowhere near as severe as it is at the higher frequencies.

We have also shown that during typical summer daytime propagation conditions, field strength enhancements of 3 to 30 dB (depending on range) can be obtained by properly exciting the whispering-gallery propagation mode.

Appendix

COMPARISON OF SIMPLIFIED APPROXIMATE THEORY WITH MODE-THEORY COMPUTER CALCULATIONS

It is the purpose of this appendix to compare some field strength calculations, using

$$E_V \sim 51.7 - 10 \log(a \sin D/a) - \alpha D + HGF \ dB\mu V/m/kW , \qquad (12)$$

with those calculated by using computer programs based on waveguide mode theory.

Figures A-1 and A-2 are two 26.1 kHz daytime field strength versus distance curves from Moler and Bickel.[48] The mode constants (eigenangles, attenuation rate, phase velocity, and excitation factors) were calculated as a function of distance and direction of propagation from the transmitter using the Naval Ocean Systems Center (NOSC) developed MODESRCH computer program. (For background and specific details, see references 17 and 49 through 53.) The MODESRCH program input variables are the ionospheric electron densities and collision frequencies appropriate to the time of day and location, the surface conductivity, the geomagnetic dip angle, flux density, azimuth with respect to the direction of propagation, and the radio frequency.

Figure A-1 is a plot of the typical daytime field strength as a function of distance for transmitter heights of 70,000 to 130,000 ft. Figure A-2 presents the vertical electric field strength at sea level as a function of distance for both east-west (EW) and west-east (WE) propagation in a spread debris nuclear environment. The transmitting antenna is located at a height of 80,000 ft. Because the nuclear-perturbed ionosphere is isotropic, this curve represents the field strength with distance variation for all directions of propagation.

For typical daytime propagation conditions, the ionospheric conductivity gradient $\ell \sim 3$ km.[33] For the more lossy disturbed environments, a more representative value of ℓ is 4 km.[54] Employing these values of ℓ in

$$\alpha \sim 13.4(\ell/\lambda)^u = 13.4\left(\frac{\ell f_{kHz}}{300}\right)^u \ dB/Mm \qquad (18)$$

with u = 1 results in 26.1 kHz attenuation rates of 3.5 dB/Mm for ℓ = 3 km and 4.7 dB/Mm for ℓ = 4 km.

The circles in figures A-1 and A-2 are the field strengths calculated from the simplified approximate theory (equations (12) and (18)). Note that the agreement between the two sets of calculations is excellent.

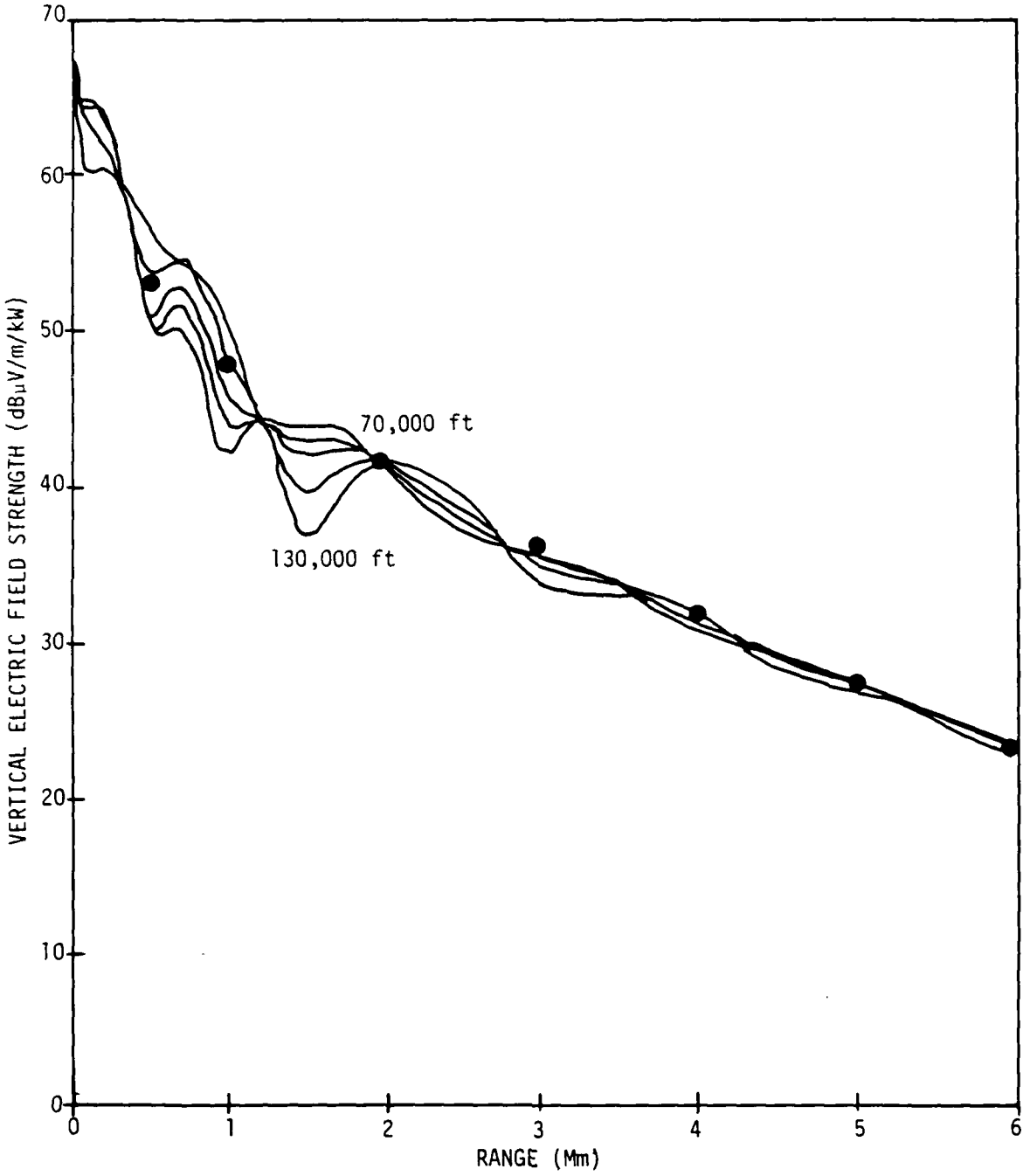

Figure A-1. Predicted Field Strength Versus Range for 26.1 kHz Transmissions From 70, 80, 90, 110, and 130 Thousand Feet

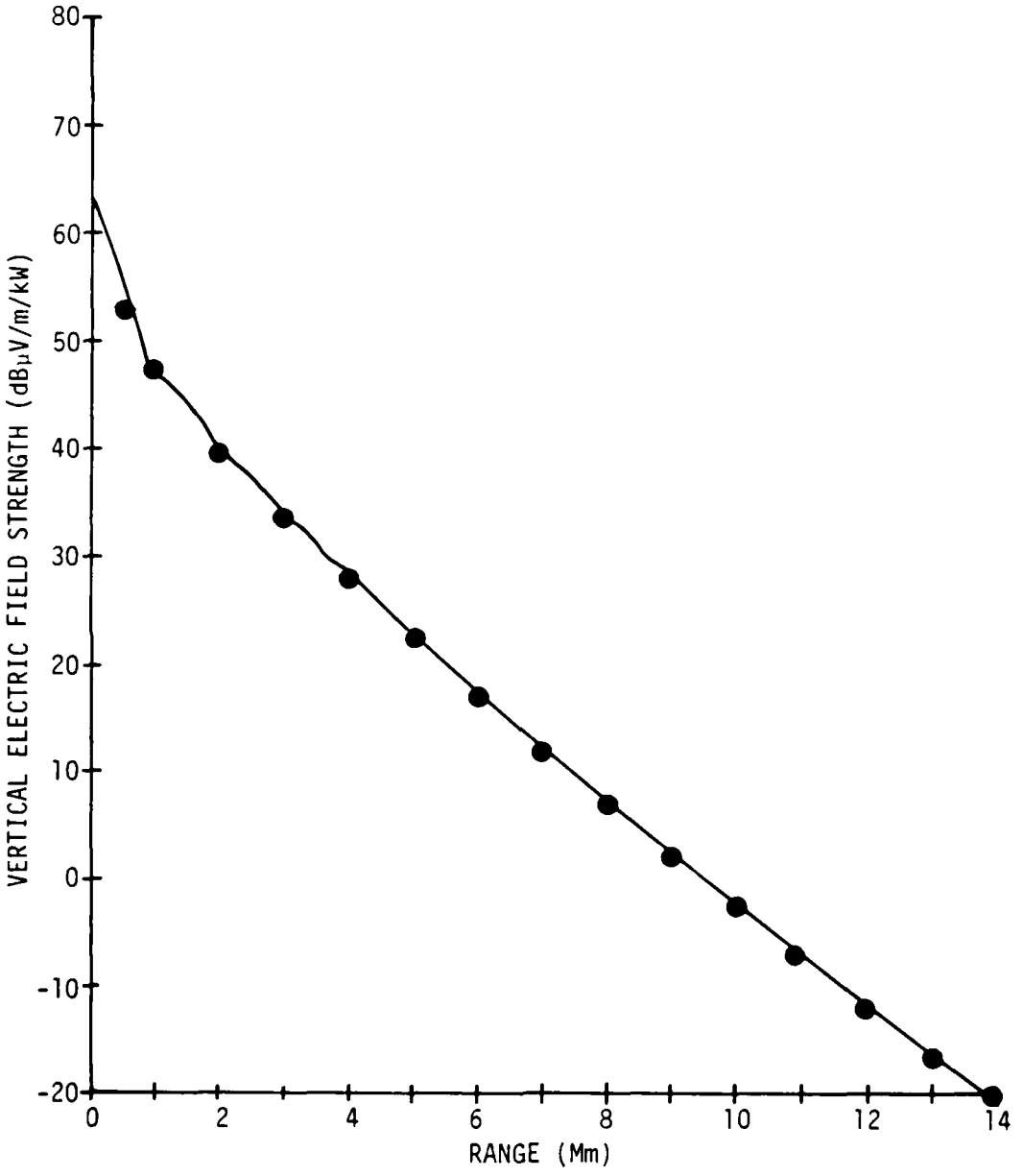

Figure A-2. Predicted Field Strength Versus Range for 26.1 kHz Transmissions in a Spread Debris Nuclear Environment

Figures A-3 through A-7 are Pappert's range plots[17] for frequencies of 100, 150, 200, 250, and 300 kHz. These calculations were made by using the lower extremities of the GE-TEMPO ambient day profile.[55] On each plot are curves for ground-to-ground transmission for transmitter and receiver at 30 km and for transmitter and receiver at 50 km. The null in the ground-to-ground transmission curves that, depending on frequency, falls in the range from about 800 to 1400 km is a manifestation of the groundwave and first hop skywave interference null. Even up through 300 kHz the ground-to-ground curves show relatively little modal structure, indicating that only a few modes are required for that configuration. The mode structure is considerably more complicated for the elevated transmitter and receiver cases.[17] The number of modes utilized ranged from a dozen at 100 kHz to 28 at 300 kHz. Minimum modal attenuation rates ranged from about 7.7 dB/Mm at 100 kHz to about 19 dB/Mm at 300 kHz.

Also shown in figures A-3 through A-7 are the simplified approximate theory ground-to-ground transmission results (equation (12)). For these calculations, only one mode has been assumed. With the exception of the groundwave and first hop skywave interference null, the agreement between the two sets of calculations is remarkably good.

The 219 kHz 1.6 Mm range field strength value (normalized to a transmitter radiated power of 1 kW) measured during the May 1972 whispering-gallery experiment[8,9] is also plotted on the 200 and 250 kHz plots (figures A-5 and A-6). Note that the measured value is very close to the 30 km-to-30 km predicted values.

A comparison of the simplified approximate theory with Pappert's[17] 150 kHz 50 km-to-50 km results for both the GE-TEMPO[55] and Deek's[56] ambient daytime ionospheric conductivity profiles is shown in figure A-8. The HGF assumed is 10 dB (figure 9) and the single-mode attenuation rates employed are 10 dB/Mm for the Deek's profile and 11.5 dB/Mm for the GE-TEMPO profile.[55] On the average, the agreement is quite good considering that only one mode was assumed for the simplified approximate-theory calculations.

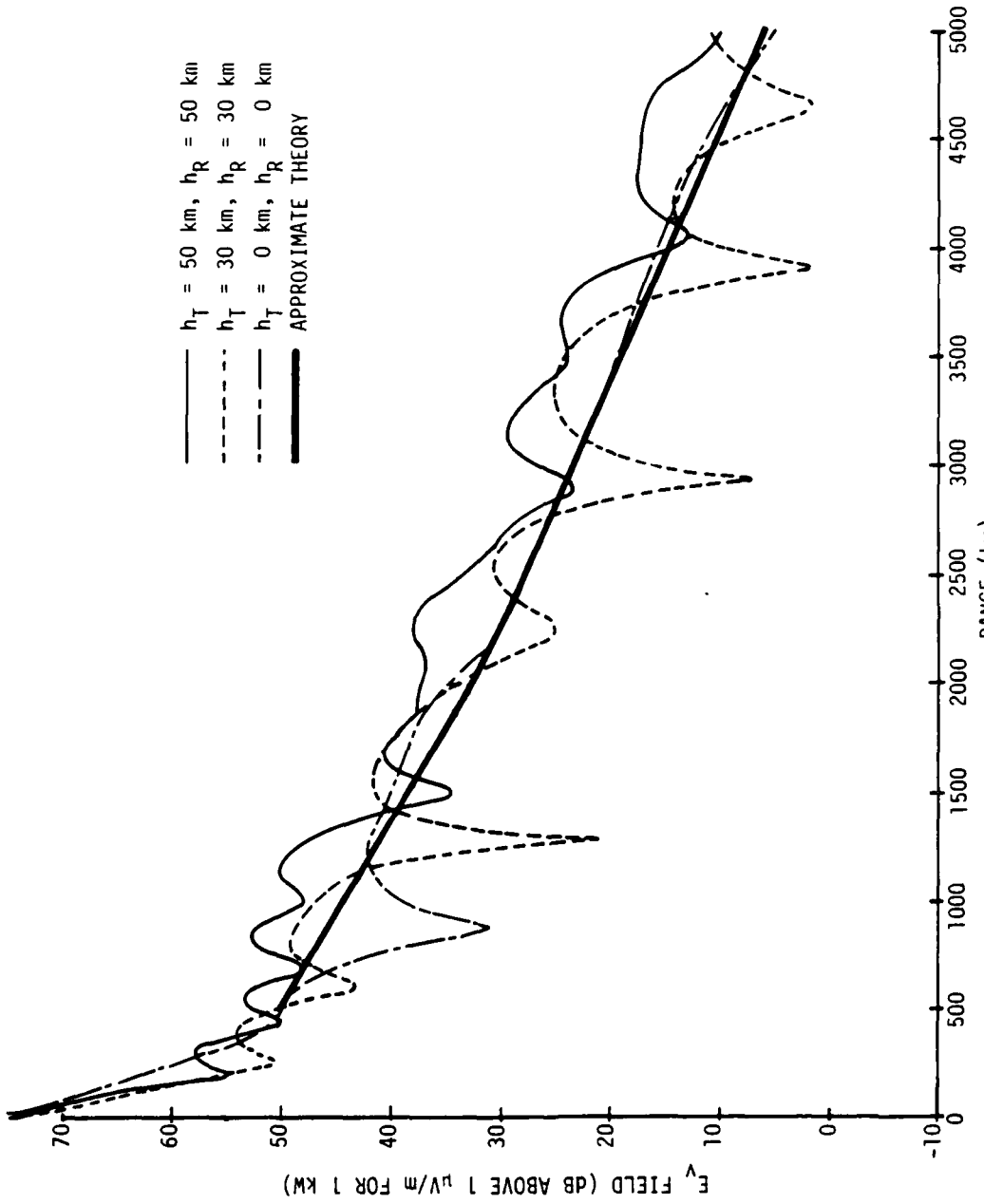

Figure A-3. Predicted 100 kHz Range Plots for GE-TEMPO Daytime Profile

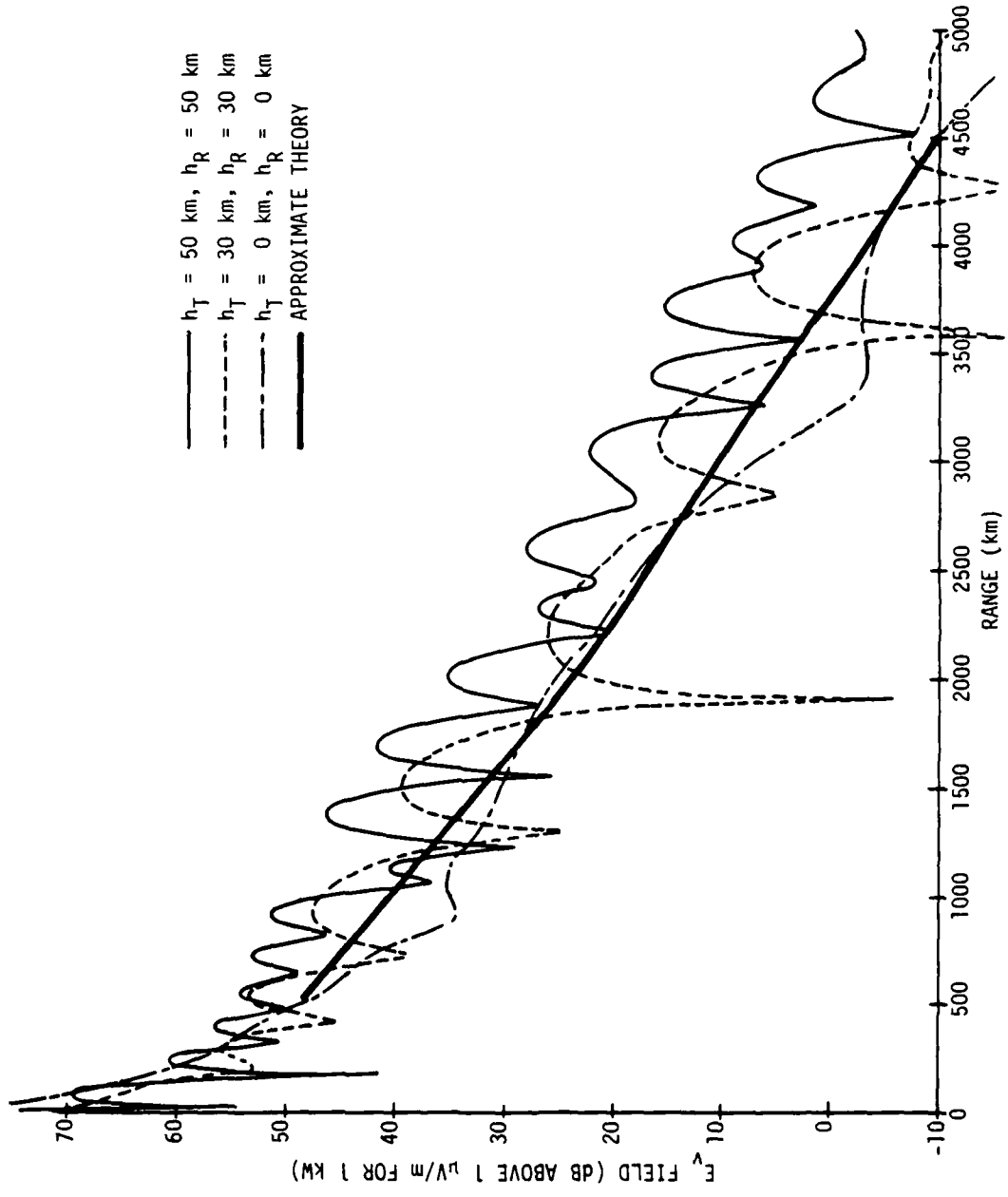

Figure A-4. Predicted 150 kHz Range Plots for GE-TEMPO Daytime Profile

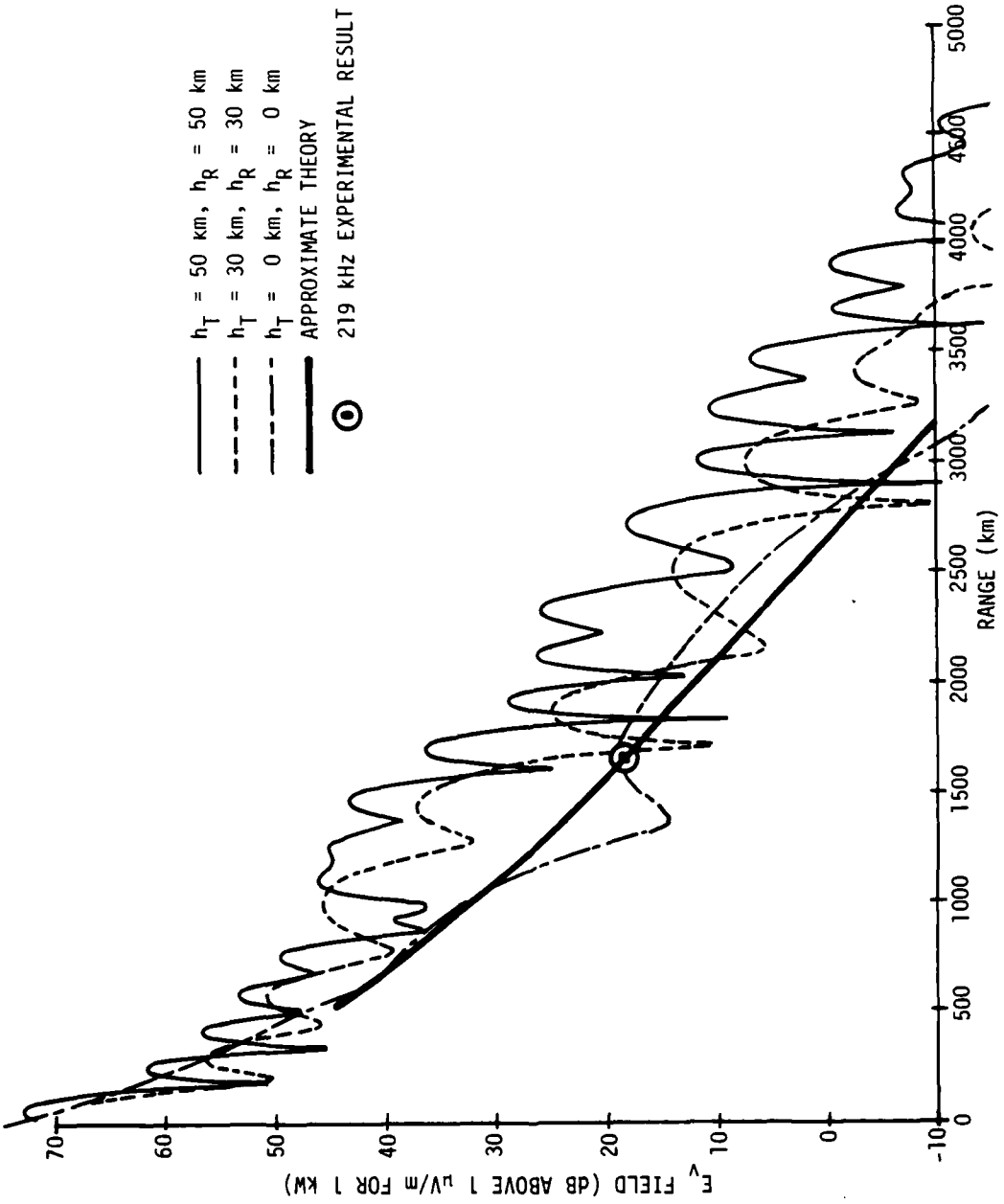

Figure A-5. Predicted 200 kHz Range Plots for GE-TEMPO Daytime Profile

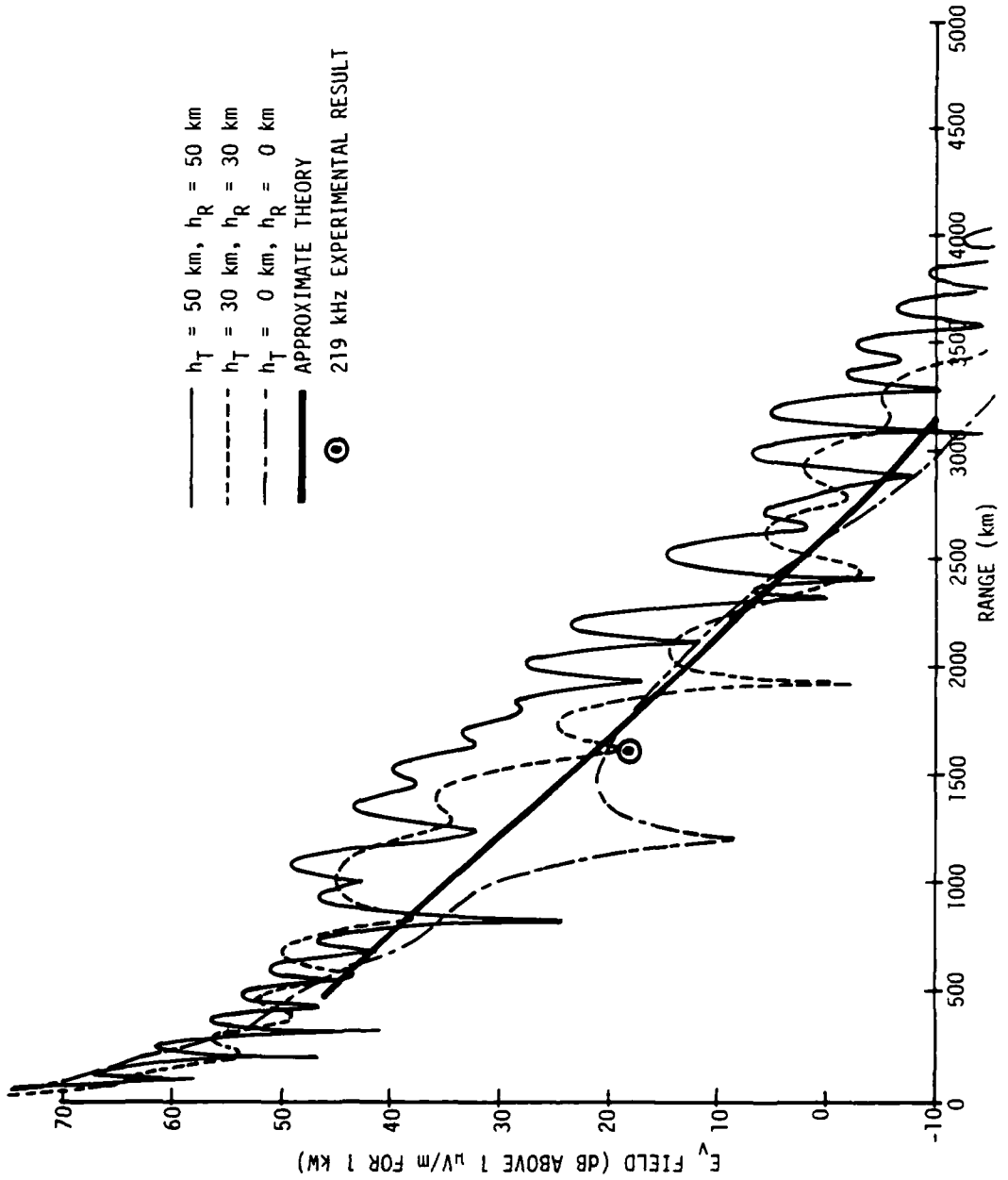

Figure A-6. Predicted 250 kHz Range Plots for GE-TEMPO Daytime Profile

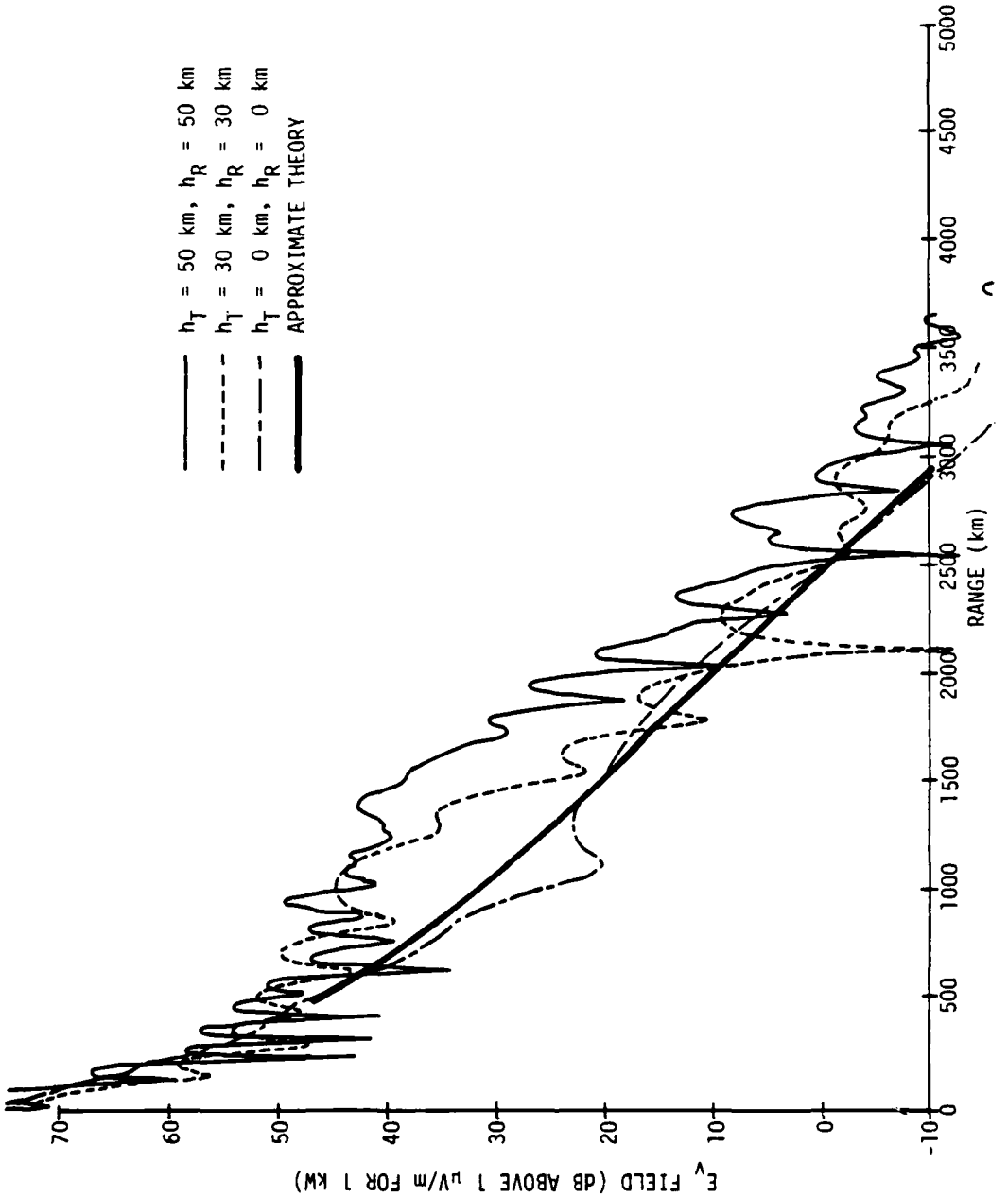

Figure A-7. Predicted 300 kHz Range Plots for GE-TEMPO Daytime Profile

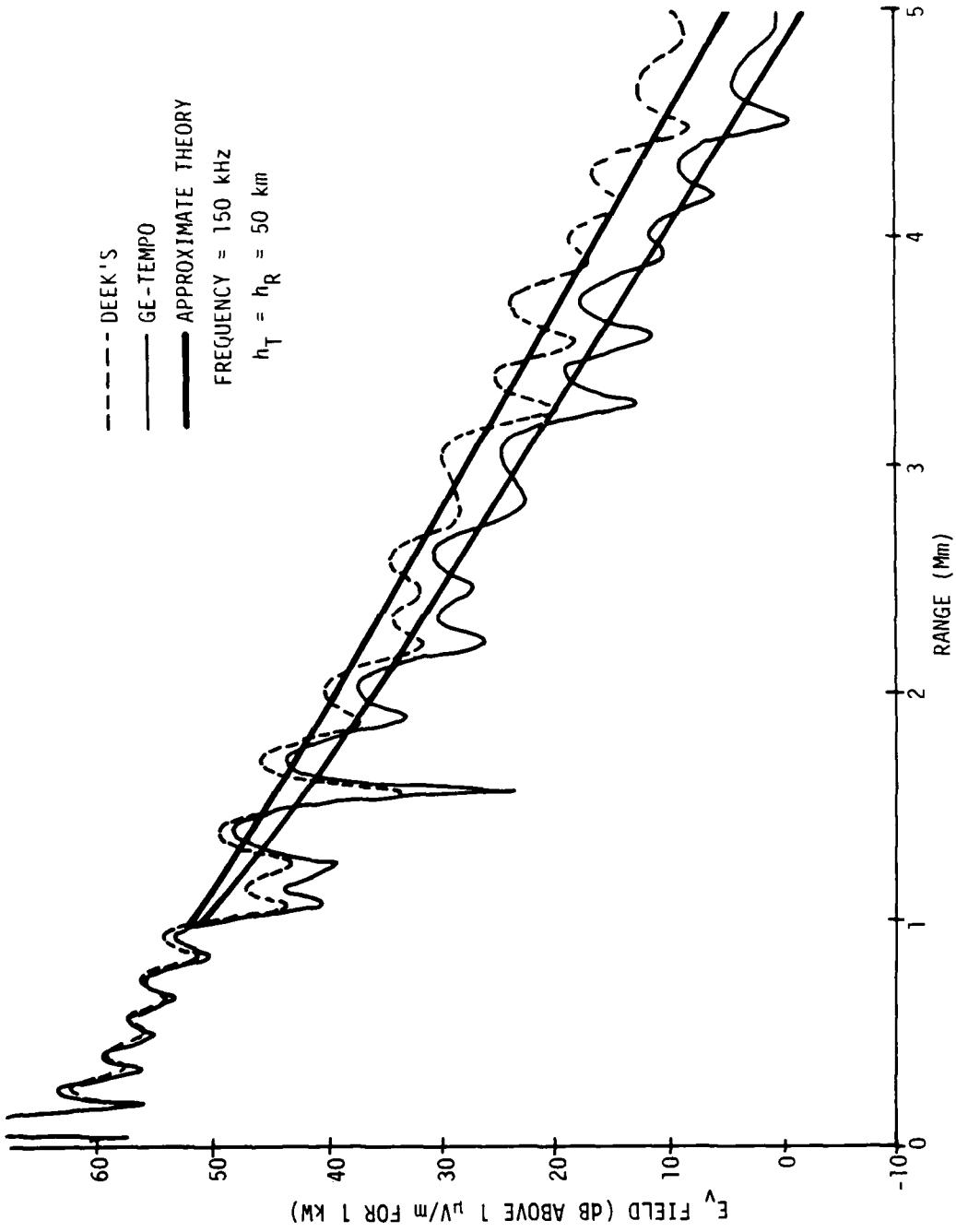

Figure A-8. 150 kHz Comparison for Deek's and GE-TEMPO Profiles ($h_T = h_R$ = 50 km)

REFERENCES

1. Lord Rayleigh, Theory of Sound, Second edition, Macmillan, London, 1896 (reprinted, Dover Publications, 1945).

2. Lord Rayleigh, "The Problem of the Whispering Gallery," Philosophical Magazine, vol. 20, 1910, pp. 1001-1004.

3. Lord Rayleigh, "Further Applications of Bessel Functions of High Order to the Whispering Gallery and Allied Problems," Philosophical Magazine, vol. 27, 1914, pp. 100-109.

4. W. H. Menke and P. G. Richards, "Crust-Mantle Whispering Gallery Phases: A Deterministic Model of Teleseismic P_n Wave Propagation," Journal of Geophysical Research, vol. 85, no. B10, October 10, 1980, pp. 5416-5422.

5. K. G. Budden and H. G. Martin, "The Ionosphere as a Whispering Gallery," Proceedings Royal Society, vol. A265, 1962, pp. 554-569.

6. J. R. Wait, "A New Approach to the Mode Theory of VLF Propagation," Journal of Research, National Bureau of Standards, vol. 65D, no. 1, 1961, pp. 37-46.

7. J. R. Wait, "The Whispering Gallery Nature of the Earth-Ionosphere Waveguide at VLF," IEEE Transactions on Antennas and Propagation, vol. AP-15, 1967, pp. 580-581.

8. J. I. Videberg and G. S. Sales, "Long Range Survivable MF Radio Communication Study Using High Altitude Whispering Gallery Modes," AFCRL Technical Report 73-0552, Air Force Cambridge Research Laboratories, Hanscom Field, MA, 28 August 1973.

9. C. R. Roberts, "D-Layer Whispering Gallery Propagation Experiment," AFCRL LDF 5-71, prepared by General Electric Co. for Air Force Cambridge Research Laboratories, Hanscom Field, MA, May 1973.

10. J. R. Johler, "Concerning Limitations and Further Corrections to Geometrical-Optical Theory for LF, VLF Propagation Between the Ionosphere and Ground," Radio Science, vol. 68D, no. 1, 1964, pp. 67-78.

11. J. R. Wait, "A Diffraction Theory of LF Skywave Propagation," Journal of Geophysical Research, vol. 66, no. 6, 1971, pp. 1713-1724.

12. L. A. Berry, "Wave Hop Theory of Long Distance Propagation of Low Frequency Radio Waves," Radio Science, vol. 68D, no. 12, 1964, pp. 1275-1284.

13. L. A. Berry and M. E. Chrisman, "The Path Integrals of LF-VLF Wave Hop Theory," Radio Science, vol. 69D, no. 11, 1965, pp. 1469-1480.

14. L. A. Berry, G. Gonzalez, and J. Lloyd, "Wave-Hop Series for an Anisotropic Ionosphere," Radio Science, vol. 4, no. 11, 1969, pp. 1025-1027.

15. L. A. Berry and J. E. Herman, "A Wave Hop Propagation Program for an Anisotropic Ionosphere," ITS Research Report 11, Institute for Telecommunication Sciences, Boulder, CO, 1971.

16. P. H. M. Campbell and T. B. Jones, "Low Frequency Radio Propagation at High Latitudes," IEEE Conference Publication No. 169, Antennas and Propagation, 1978, pp. 47-50.

17. R. A. Pappert, "LF Daytime Earth Ionosphere Waveguide Calculations," NOSC Technical Report 647, Naval Ocean Systems Center, San Diego, CA, January 1981.

18. J. Galejs, Terrestrial Propagation of Long Electromagnetic Waves, Chapter 9, Pergamon Press, Oxford, 1972.

19. J. R. Wait, "Concise Theory of Radio Transmission in the Earth-Ionosphere Wave Guide," Reviews of Geophysics and Space Physics, vol. 16, no. 3, August 1978, pp. 320-326.

20. J. R. Wait, "Theory of the Terrestrial Propagation of VLF Electromagnetic Waves," ELF-VLF Radio Wave Propagation, edited by J. Holtet, D. Reidel Publishing Co., Dordrecht, Holland, 1974, pp. 129-147.

21. J. R. Wait, Electromagnetic Waves in Stratified Media, Pergamon Press, Oxford, 1970.

22. J. C. P. Miller, The Airy Integral, British Association Mathematical Tables, Part-Volume B, University Press, Cambridge, 1946.

23. M. Abramowitz and I. A. Stegun, Handbook of Mathematical Functions, National Bureau of Standards, Washington, DC, p. 446, 1964.

24. R. R. Rutherford, "Extended Range Analysis for Normal and Nuclear Environments," Task A-2 and Task A-3, Final Report, GE 80 TMP-52, General Electric-TEMPO, Santa Barbara, CA, October 1980.

25. R. R. Rutherford and B. Gambill, "VLF/LF/MF Computer Code Modification," Task A-1, Final Report, GE 80 TMP-32, General Electric-TEMPO, Santa Barbara, CA, June 1980.

26. R. R. Rutherford and B. Gambill, "Analysis of LF Propagation With Parametric Ionospheric Profiles," Task A-4, Final Report, GE 80 TMP-38, General Electric-TEMPO, Santa Barbara, CA, August 1980.

27. "LF Signal Propagation Analysis Program," Final Report, Tasks 1, 2, and 3, General Electric Company, Santa Barbara, CA, 30 June 1978.

28. "LF Signal Propagation Analysis Program," Final Report, Addendum, Task 4, General Electric Company, Santa Barbara, CA, 31 October 1978.

29. "LF Signal Propagation Analysis Program," Final Report, Task 7, General Electric Company, Santa Barbara, CA, August 1979.

30. R. R. Rutherford, "WEDCOM IV: A FORTRAN Code for the Calculation of ELF, VLF, and LF Propagation in a Nuclear Environment," Vol. III, General Electric-TEMPO, Santa Barbara, CA, 1 November 1978, DNA 4422T-3.

31. K. Davies, Ionospheric Radio Propagation, National Bureau of Standards Monograph 80, April 1, 1965, Superintendent of Documents, U. S. Government Printing Office, Washington, DC, p. 439.

32. J. S. Belrose, W. L. Hatton, C. A. McKerrow, and R. S. Thain, "The Engineering of Communications Systems for Low Radio Frequencies," Proceedings of the IRE, vol. 47, 1959, p. 661.

33. A. D. Watt, VLF Radio Engineering, Pergamon Press, Oxford, 1967.

34-39. B. S. Westott, "Ionospheric Reflection Processes for Long Radio Waves," Journal of Atmospheric and Terrestrial Physics, Part I, vol. 24, 1962, pp. 385-399; Part II, vol. 24, 1962, pp. 619-631; Part III, vol. 24, 1962, pp. 701-713; Part IV, vol. 24, 1962, pp. 921-936; Part V, vol. 26, 1964, pp. 341-350.

40. R. A. Pappert and L. R. Shockey, "Ionospheric Reflection and Absorption Properties of Normal Modes at ELF," NOSC Interim Report No. 772, Naval Ocean Systems Center, San Diego, CA, September 1977.

41. E. C. Field and R. D. Engel, "The Detection of Daytime Nuclear Bursts Below 150 km by Prompt VLF Phase Anomalies," Proceedings of the IEEE, vol. 53, 1965, pp. 2009-2017.

42. J. A. Pierce, "Sky-Wave Field Intensity I: Low and Very Low Frequencies," Cruft Laboratory Technical Report No. 158, Harvard University, 1952.

43. "World Distribution and Characteristics of Atmospheric Radio Noise," International Radio Consultative Committee (C.C.I.R.) Report 322, International Telecommunications Union, Geneva, 1964.

44. J. A. Ferguson, "Ionospheric Profiles for Predicting Nighttime VLF/LF Propagation," NOSC Technical Report No. 530, Naval Ocean Systems Center, San Diego, CA, 25 February 1980.

45. C. B. Brookes, Jr., J. H. McCabe, and F. J. Rhoads, "Theoretical Multimode Propagation Predictions," NRL Report No. 6663, Naval Research Laboratory, Washington, DC, 1 December 1967.

46. J. R. Wait and K. P. Spies, "Characteristics of the Earth-Ionosphere Waveguide for VLF Radio Waves," NBS Technical Note No. 300, National Bureau of Standards, Washington, DC, 30 December 1964.

47. E. Bahar, "Computations of the Transmission and Reflection Scattering Coefficients in an Irregular Spheroidal Model of the Earth-Ionosphere Waveguide," Radio Science, vol. 15, no. 5, 1980, pp. 987-1000.

48. W. F. Moler and J. E. Bickel, "Theoretical Study of Diversity Gains at VLF," presented at the Survivable and Reconstitutable VLF Communications Technical Coordination Meeting, held at the MITRE Corporation, McLean, VA, 23 September 1980.

49. R. A. Pappert, W. F. Moler, and L. R. Shockey, "A FORTRAN Program for Waveguide Propagation Which Allows for Both Vertical and Horizontal Dipole Excitation," NOSC Interim Report No. 702, Naval Ocean Systems Center, San Diego, CA, June 1970.

50. R. A. Pappert and L. R. Shockey, "WKB Mode Summing Programs for VLF/ELF Antennas of Arbitrary Length, Shape, and Elevation," NOSC Interim Report No. 713, Naval Ocean Systems Center, San Diego, CA, June 1971.

51. D. B. Morfitt and C. H. Shellman, "MODESRCH, An Improved Computer Program for Obtaining ELF/VLF/LF Mode Constants in an Earth-Ionosphere Waveguide," NOSC Interim Report No. 77T, Naval Ocean Systems Center, San Diego, CA, October 1976.

52. J. A. Ferguson, "An Aid for Using the NELC WAVEGUIDE Program," NELC Technical Note 2480, Naval Electronics Laboratory Center, San Diego, CA, September 1973.

53. R. A. Pappert, "A Numerical Study of VLF Mode Structure and Polarization Below an Anisotropic Ionosphere," Radio Science, vol. 3, no. 3, 1968, pp. 219-233.

54. W. F. Moler and R. A. Pappert, "Effects of Ionospheric Reflection Height and Ground Conductivity on Earth-Ionosphere Waveguide Mode and Ground-Wave Attenuation Rates," NOSC Technical Report No. 561, Naval Ocean Systems Center, San Diego, CA, June 1980.

55. W. Knapp, "Reaction Rate, Collision Frequency, and Ambient Ionospheric Models for Use in Studies of Radio Propagation for Nuclear Environment," General Electric-TEMPO Report 66 TMP-82, Santa Barbara, CA, March 1967.

56. D. G. Deek, "D-Region Electron Distributions in Middle Latitudes Deduced From the Reflection of Long Radio Waves," Proceedings Royal Society, vol. A291, 1966, pp. 413-437.

INITIAL DISTRIBUTION LIST

Addressee	No. of Copies
DARPA	3
DTIC	15
ONR (Code 425GG (J. Heacock), 428IO (R. G. Joiner))	2
ONR Branch Office, Chicago, (Dr. Forrest L. Dowling)	1
ASN (T. P. Quinn (for C^3), J. Hull (Rm 5E 779)	2
NRL (Library, Dr. J. R. Davis (Code 7550), Dr. Frank Kelly)	3
NOSC (Library, R. A. Pappart, D. G. Morfitt, J. A. Ferguson, F. P. Snyder, C. F. Ramstedt, P. Hansen, K. Grauer, W. Hart)	9
NAVELECSYSCOM (PME 110-11 (Dr. G. Brunhart), PME 110-X1 (Dr. Bodo Kruger), PME 110)	3
NAVAL SURFACE WEAPONS CENTER, WHITE OAK LAB. (J. J. Holmes, M. B. Kraichman, P. Wessel, K. Bishop, R. Brown, J. Cunningham, B. DeSavage, Library)	8
DWTNSRDC ANNA (W. Andahazy, F. E. Baker, P. Field, D. Everstine, B. Hood, D. Nixon)	6
NAVPGSCOL, MONTEREY (O. Heinz, P. Moose, Library)	3
NCSC (K. R. Allen, R. H. Clark, M. J. Wynn, M. Cooper, Library)	5
DIRECTOR, DEFENSE NUCLEAR AGENCY, RAAE, DDST, RAEV	3
R&D Associates, P.O. Box 9695, Marina del Rey, CA 90291 (C. Greifinger, P.Greifinger)	2
Pacific-Sierra Research Corp., 1456 Cloverfield Boulevard, Santa Monica, CA 90404 (E. C. Field)	1
Johns Hopkins University, Applied Physics Laboratory, Laurel, MD 20810 (L. Hart, J. Giannini, H. Ko, I Sugai)	4
University of California, Scripps Institute of Oceanography (C. S. Cox (Code A-030), H. G. Booker, J. Filloux)	4
Lockheed Palo Alto Research Laboratory (W. Imhof, J. B. Reagan, E. E. Gaines, R. C. Gunton, R. E. Meyerott)	5
University of Texas, Geomagnetics and Electrical Geoscience Laboratory (F. X. Bostick, Jr.)	1
COMMANDER, AIR FORCE GEOPHYSICS LABORATORY (J. Aarons)	1
COMMANDER, ROME AIR DEVELOPMENT CENTER (J. P. Turtle, J. E. Rasmussen, W. I. Klemetti, P. A. Kossey, E. F. Altschuler)	5
Applied Science Associates, Inc., (Dr. Gary S. Brown) 105 E. Chatham St., Apex, NC 27502	1
Computer Sciences Corp., Falls Church, VA 22046 (D. Blumberg, Senator R. Mellenberg, R. Heppe, F. L. Eisenbarth)	4
MIT Lincoln Labs. (M. L. Burrows, D. P. White, D. K. Willim, S. L. Bernstein, I. Richer)	5
Electromagnetic Sciences Lab. SRI International, Menlo Park, CA 94025 (Dr. David M. Bubenik)	1
Communications Research Centre (Dr. John S. Belrose) P.O. Box 11490, Station "H" Shirley Bay, Ottawa, Ontario, Canada K2H8S2	1
West Virginia University, Electrical Eng. Dept. (Prof. C. A. Balanis)	1
Dr. Joseph P. deBettencourt, 18 Sterling St., West Newton, MA 02165	1
Dr. Marty Abromavage, IITRE, Div. E., 10W 35th St., Chicago, IL 60616	1
Mr. Larry Ball, U.S. Dept. of Energy NURE Project Office, P.O. Box 2567, Grand Junction, CO 81502	1

INITIAL DISTRIBUTION LIST (Cont'd)

Addressee	No. of Copies
STATE DEPARTMENT ACDA MA-AT, Rm. 5499, Washington, DC 20451 (ADM T. Davies, R. Booth, N. Carrera)	3
GTE Sylvania, (R. Row, D. Boots, D. Esten) 189 B. St. Needham, MA 02194	3
HARVARD UNIVERSITY, Gordon McKay Lab. (Prof. R. W. P. King, Prof. T. T. Wu)	2
University of Rhode Island, Dept. of Electrical Engineering (Prof. C. Polk)	1
Pheonix Corporation (Dr. Robert D. Regan), 1600 Anderson Rd., McLean, VA 22101	1
University of Nebraska, Electrical Engineering Dept., (Prof. E. Bahar)	1
University of Toronto, EE Dept. (Prof. Keith Balmain)	1
NOAA/ERL (Dr. Donald E. Barrick)	1
University of Colorado, EE Dept. (Prof. Petr Beckmann)	1
Geophysical Observatory, Physics & Eng. Lab. DSIR Christchurch, New Zealand (Dr. Richard Barr)	1
U.S. Army Electronic Command Headquarters, Fort Monmouth, NJ (Mr. Morris Acker)	1
General Electric Co., (C. Zierdt, A. Steinmayer) 3198 Chestnut St., Philadelphia, PA 19101	2
University of Arizona, Elec. Eng. Dept., Bldg. 20 (Prof. J. W. Wait) Tucson, AZ 85721	1
U.S. NAVAL ACADEMY, Dept. of Applied Science (Dr. Frank L. Chi)	1
Stanford University, Radioscience Laboratory (Dr. Anthony Fraser-Smith), Durand Bldg., Rm. 205	1
Stanford University, Stanford Electronics Laboratory (Prof. Bob Helliwell)	1
Colorado School of Mines, Department of Geophysics (Prof. A. Kaufman)	1
Prof. George V. Keller, Chairman, Group Seven, Inc., Irongate II, Executive Plaza, 777 So. Wadsworth Blvd., Lakewood, CO 80226	1
NOAA, Pacific Marine Environ. Lab. (Dr. Jim Larsen)	1
MIT, Dept. of Earth/Planetary Sciences, Bldg. 54-314 (Prof. Gene Simmons)	1
Colorado School of Mines (Dr. C. Stoyer)	1
University of Victoria, (Prof. J. Weaver) Victoria, B.C. V8W 2Y2 Canada	1
Mr. Donald Clark, c/o Naval Security Group Command, 3801 Nebraska Ave., NW, Washington, DC 20390	1
Prof. R. L. Dube, 13 Fairview Rd., Wilbraham, MA 01095	1
U.S. Geological Survey, Rm. 1244 (Dr. Frank C. Frischknecht) Denver, CO 80225	1
Mr. Larry Ginsberg, Mitre Corp., 1820 Dolly Madison Bldg. McLean, VA 22102	1
Dr. Robert Morgan, Rt. 1, Box 187, Cedaredge, CO 81413	1
Mr. A. D. Watt, Rt. 1, Box 183½, Cedaredge, CO 81413	1
Dr. E. L. Maxwell, Atmospheric Sciences Dept., Colorado State University, Fort Collins, CO	1
Mr. Al Morrison, Purvis Systems, 3420 Kenyon St., Suite 130, San Diego, CA 92110	1

INITIAL DISTRIBUTION LIST (Cont'd)

Addressee	No. of Copies
NDRE, Division for Electronics (Dr. Trygve Larsen) P.O. Box 25, Kjeller, Norway	1
Belden Corp., Technical Research Center (Mr. Douglas O'Brien) Geneva, Illinois	1
University of Pennsylvania (Dr. Ralph Showers) Moore School of Elec. Eng., Philadelphia, PA 19174	1
University of Houston, Director, Dept of Elec. Eng. (Prof. Liang C. Shen)	1
The University of Connecticut, Physics Dept., (Prof. O. R. Gilliam), Storrs, CT 06268	1
Dr. David J. Thomson, Defence Research Establishment Pacific, F.M.O., Victoria, B.C., Canada	1
Dr. Robert Hansen, Box 215, Tarzana, CA 91356	1
The University of Kansas, Remote Sensing Laboratory (Prof. R. K. Moore) Center for Research, Inc., Lawrence, Kansas	1
University of Wisconsin, Dept. of Elec. Eng. (Prof. R. J. King)	1
OT/ITS U.S. Dept. of Commerce (Dr. David A. Hill), Boulder, CO	1
Office of Telecommunications, Inst. for Telecommunications Services (Dr. Douglas D. Crombie, Director), Boulder, CO	1
University of Colorado, Dept. of Electrical Eng. (Prof. David C. Chang)	1
Dr. K. P. Spies, ITS/NTIA, U.S. Dept. of Commerce	1
The University of Connecticut, Dept. of Electrical Eng. & Computer Sci., Storrs, CT (Prof. Clarence Schultz, Prof. Mahmond A. Melehy)	2
Dr. Richard G. Geyer, 670 S. Estes St., Lakewood, CO	1
University of California, Lawrence Livermore Lab., (R. J. Lytle, E. K. Miller)	2
Kings College, Radiophysics Group (Prof. D. Llanwyn-Jones) Strand, London WC2R 2LS, England	1
Istituto di Elettrotechnica, Facotta di Ingegneria (Prof. Giorgio Tacconi) Viale Cambiaso 6, 16145 Genova, Italy	1
Universite des Sciences de Lille (Prof. R. Gabillard) B.P. 36-59650 Villeneuve D'Ascq, Lille, France	1
Arthur D. Litte, Inc., (Dr. A. G. Emslie, Dr. R. L. Lagace, R&D Div., Acorn Park, Cambridge, MA 02140	1
University of Colorado, Dept. of Electrical Eng. (Prof. S. W. Maley)	1
University of Washington, EE Dept. (Prof. A. Ishimaru) Seattle	1
Dr. Svante Westerland, Kiruna Geofysiska Institute S981 01 Kiruna 1, Sweden	1
Dr. Harry C. Koons, The aerospace Corp., P.O. Box 92957, Los Angeles, CA 90009	1
Dr. Albert Essmann, Hoogewinkel 46, 23 Kiel 1, West Germany	1
Glenn S. Smith, School of Elec. Eng. Georgia Tech. Atlanta, GA	1
Dr. T. Lee, CIRES, Campus Box 449, University of Colorado	1
Dr. Jack Williams, RCA Camden, Mail Stop 1-2, Camden, NJ 08102	1
Dr. Joseph Czika, Science Applications, Inc., 840 Westpark Dr. McLean, VA 22101	1
Mr. Arnie Farstad, 390 So. 69th St., Boulder, CO 80303	1

INITIAL DISTRIBUTION LIST (Cont'd)

Addressee	No. of Copies
NATO SACLANT ASW CENTER (Library)	1
USGS, Branch of Electromagnetism and Geomagnetism (Dr. James Towle) Denver, CO	1
NOAA, Pacific Maine Environ. Lab. (Dr. Jim Larsen)	1
University of Texas at Dallas, Geosciences Division, (Dr. Mark Landisman)	1
University of Wisconsin, Lewis G. Weeks Hall, Dept. of Geology and Geophysics (Dr. C. S. Clay)	1
DCA/CCTC, Def Communication Agency, Code C672 (Dr. Frank Moore)	1
Argonne National Laboratory, Bldg. 12 (Dr. Tony Vallentino)	1
IITRE, Div. E, Chicago (Dr. Marty Abromavage)	1
The University of Manitoba, Elec. Eng. Dept. (Prof. A. Mohsen)	1
Mr. Jerry Pucillo, Analytical Systems, Engineering Corp., Newport, RI 02840	1
Dr. Misac N. Nabighian, Newmont Exploration Ltd., Tuscon	1
Dr. Fred Raab, Pohemus, P.O. Box 298, Essex Junction, VT 05452	1
Dr. Louis H. Rorden, President, Develco, Inc., 404 Tasman Dr. Sunnyvale, CA 94086	1
Dr. D. D. Snyder, EDCON, 345 South Untion Blvd, Lakewood, CO	1
Dr. Eivind Trane, NDRE, P.O. Box 25, 2007 Kjeller, Norway	1
RCA David Sarnoff Research Center (K. Powers, J. Zennel, L. Stetz, H. Staras)	4
University of Illinois, Aeronomy Laboratory (Prof. C. F. Sechrist)	1
Dr. Cullen M. Crain, Rand Corp., Santa Monica	1
Radioastronomisches Institute der Universität Bonn (Dr. H. Volland), 5300 Bonn-Endenich, Auf dem Hiigel 71 West Germany	1
Dr. John P. Wikswo, Jr., P.O. Box 120062 Acklen Station, Nashville	1
Mr. Lars Brock-Nannestad, DDRB Osterbrogades Kaserne, 2100 Copenhagen O, Denmark	1
Institut de Physique du Globe (Dr. Edonard Selzer) 11 Quai St., Bernard, Tour 24 Paris Ve, France	1
Elektrophysikalisches Institut (Dr. Herbert König) Technische Hochschule, Arcisstrasse 21, 8 Munich 2, West Germany	1
Raytheon Company (Dr. Mario Grossi) Portsmouth, RI	1
NISC, Code 00W (Mr. M. A. Koontz) Washington, DC	1
Polytechnic Institute of Brooklyn (Prof. Leo Felsen)	1
NOAA/ERL (Dr. Earl E. Gossard) R45X7, Boulder, CO 80302	1
Dr. George H. Hagn, SRI-Washington, Rosslyn Plaza, Arlington	1
NOAA/ERL (Dr. C. Gordon Little) R45	1
Goddard Space Flight Ctr. (Dr. S. H. Durrani) Code 950	1
ITS, Office of Telecom (Dr. Ken Steele) Boulder, CO 80302	1
NTIA/ITS, U.S. Dept. of Commerce (Dr. A. D. Spaulding)	1
Stanford University, Elec. Eng. Dept. (Dr. O. G. Villard, Jr.)	1
Dr. D. Middleton, 127 East 91st St., New York, NY 10028	1
University of California, Elec. Eng. & Computer Sci. Dept., (Prof. K. K. Mei)	1

INITIAL DISTRIBUTION LIST (Cont'd)

Addressee	No. of Copies
California Inst. of Technology, Jet Propulsion Lab., (Dr. Yahya Rahmat-Samii)	1
Raytheon Service Co. (Dr. M. Soyka) Mt. Laurel, NJ 08054	1
MITRE M/S W761 (Dr. W. Foster) McLean, VA	1
Max-Planck-Institut fur Aeromomie (Prof. P. Stubbe) 3411 Katlenburg-Lindau 3 FRG	1
University of Otago, Physics Dept. (Prof. R. L. Dowden) Dunedin, New Zealand	1
University of Leicester, Physics Dept. (Prof. T. B. Jones) Leicester, England	1
Naval Weapons Center, China Lake, Code 3814 (Dr. R. J. Dinger)	1
Dr. Claudia D. Tesche, Lutech, Inc., P.O. Box 1263, Berkeley	1
National Aeronautical Est., National Research Council, Flight Research Lab., (Dr. C. D. Harwick) Ottawa, K1AOR6, Canada	1
Colorado Research and Prediction Laboratory, Inc. (Dr. R. H. Doherty, Dr. J. R. Johler) Boulder, CO	2


DATE
ILME